8-9-2019

High Order Implementation in Integral Equations

Joshua P. Marshall

High order implementation in integral equations

By

Joshua P. Marshall

A Dissertation
Submitted to the Faculty of
Mississippi State University
in Partial Fulfillment of the Requirements
for the Degree of Doctor of Philosophy
in Computational Engineering
in the Department of Computational Engineering

Mississippi State, Mississippi

August 2019

High order implementation in integral equations

By

Joshua P. Marshall

Approved:

Manav Bhatia
(Major Professor/Graduate Coordinator)

Joseph D. Richardson
(Committee Member/Dissertation Advisor)

Michael D. Hamilton
(Committee Member)

Jeffrey L. Hensley
(Committee Member)

Jason M. Keith
Dean
Bagley College of Engineering

Name: Joshua P. Marshall

Date of Degree: August 9, 2019

Institution: Mississippi State University

Major Field: Computational Engineering

Major Professor: Manav Bhatia

Title of Study: High order implementation in integral equations

Pages of Study: 105

Candidate for Degree of Doctor of Philosophy

The present work presents a number of contributions to the areas of numerical integration, singular integrals, and boundary element methods. The first contribution is an elemental distortion technique, based on the Duffy transformation, used to improve efficiency for the numerical integration of near hypersingular integrals. Results show that this method can reduce quadrature expense by up to 75 percent over the standard Duffy transformation. The second contribution is an improvement to integration of weakly singular integrals by using regularization to smooth weakly singular integrals. Errors show that the method may reduce errors by several orders of magnitude for the same quadrature order. The final work investigated the use of regularization applied to hypersingular integrals in the context of the boundary element method in three dimensions. This work showed that by using the simple solutions technique, the BEM is reduced to a weakly singular form which directly supports numerical integration. Results support that the method is more efficient than the state-of-the-art.

Key words: singular integrals, near singular integrals, numerical integration, domain transformation, boundary element methods, Green's functions, regularization

ACKNOWLEDGEMENTS

I would like to acknowledge the committees, individuals, and organizations involved in the funding of my education. I consider myself exceptionally fortunate in that I was able to receive financial assistance from a number of sources. Throughout my education, I have never taken this for granted and realize that many students have completed their own journey with far less resources than I have had. Receiving these awards, without question, changed the trajectory of my life in an extremely positive way. My educational path would not have been possible without scholarships, Pell grants, fellowships, assistantships, and other forms of financial assistance. I will do my best to represent you all well throughout my career. I would also like to acknowledge a few friends and educators who were important along the way.

I'd like to thank my father, **Rocky Marshall**, for helping me pay for summer courses, covering miscellaneous expenses (especially during my senior year of undergrad) and also providing affordable residence for over ten years. The continuity and reliability of home has been a huge part of my success.

I'd like to thank the incredible mathematics educators from Mississippi Gulf Coast Community College: **Mr. John Miller**, **Mr. Raymond Tanner**, and **Mr. James Gilbert**. You guys made learning mathematics way more enjoyable that I ever knew it could be. I didn't realize it at the time, but I came to realize that my time learning from y'all was

absolutely essential in developing legitimate enjoyment for mathematics. You guys were basically the MGCCC all-star math team.

I'd like to thank engineering secretaries (both present and former) at the University of South Alabama: **Ms. Cathy Schwartz**, **Ms. Ronda Girardeau**, and **Ms. Brenda Poole**. You all helped me tremendously on countless occasions, in spite of having several other important things on your plate.

I'd like to thank **Dr. Gail Jefferson** for her role in my undergraduate senior project. I have a little saying that I now tell myself in the face of adversity: "I survived the rocket team, this can't possibly be harder than that." It was painful, but I came out on the other end with what feels like a few lifetimes of "lessons learned." Those lessons were infinitely more valuable than any of the engineering analysis done in my undergraduate studies. Perhaps the most important thing I learned is that our true limitations are far, far beyond what we perceive them to be.

I'd like to thank **Scott Pressnell** for his true friendship, and his above-and-beyond help with the previously mentioned undergraduate senior project. Scott still calls me regularly to tell me he had a nightmare about being back on the rocket team. I'd say poor guy, but I have them too.

I'd like to thank the 2011 iteration of the **USA-LINK committee** at the University of South Alabama for the three-year transfer scholarship that was awarded to me in 2011, despite the fact that my essay (allegedly) had a curse word in it. This award was a total game changer. Receiving this award and representing USA has been an honor.

I'd like to thank the **Gulf Coast Technology Council** (GCTC) for their gracious scholarship awarded to me in the Spring semester of 2013. You guys show continued support to the university and the local community, and the work y'all do is appreciated.

I'd like to thank the **Alabama Space Grant Consortium** for their gracious scholarship awarded to me in the Fall semester of 2013. I still use the really cool binder that you guys gave the recipients.

I'd like to thank the **Department of Mechanical Engineering** at the University of South Alabama for providing an assistantship to cover tuition costs in the Fall 2014 and Spring 2015 semesters. Graduate school would not have been in the cards for me if you guys had not come through with that.

I'd like to thank **Dr. Joseph Richardson**, **Dr. Sally Steadman**, **Dr. John Steadman**, **Dr. Vasiliy Prokhorov**, **Dr. Gail Jefferson**, **Dr. Carlos Montalvo**, **Dr. Francis Donovan**, **Dr. Francis Dougherty**, **Mr. John Miller**, and **Mr. Bobby Ghosal** for taking the time to write a recommendation letter(s) for me. If you guys had not taken the time, then I wouldn't have been able to apply for all of the funding that I received.

I'd like to thank the American Society for Engineering Education's **Science Mathematics and Research for Transformation program** (ASEE's SMART) for providing a *really* sweet fellowship that gave me a path toward a doctorate, as well as provided a path into engineering research as a career.

I'd like to thank the leadership in the Institute for Systems Engineering Research, specifically **Dr. Simon Goerger** and **Mr. Alex Baylot** for taking a chance on me as a scholar recipient for the SMART program.

I'd like to thank **Dr. Manav Bhatia**, **Dr. Jeffrey Hensley**, and **Dr. Michael Hamilton** for agreeing to serve on my committee, and providing useful feedback on this dissertation.

I'd like to thank **Dr. Manav Bhatia** for being an *excellent* graduate coordinator for the computational engineering department. I've had my fair share of experience with dealing with graduate schools, department chairs, graduate coordinators, etc, and Dr. Bhatia is simply in a tier of his own.

I'd like to thank **Cody Salter** for his comradery for the past four years. It was cool to take the same path with someone all the way from USA MSME to ERDC.

I'd like to thank **Trevin Osterman**, **Christopher Sigrest**, **Michael Rea**, and **Parker Jones**. At numerous points, you guys got up at 4AM to hit some iron with me because of my schedule.

I'd like to thank **Justin Stewart** for his exceptional friendship, particularly in the past several years.

I'd like to thank my wonderful fiancee, **Kaila Murphy** for her incredible support during the final year of my studies, and for deciding to share this life with me. The last year would have not been nearly as enjoyable without you!

Above all, I would like to thank my advisor, **Dr. Joseph D. Richardson** for his guidance, professionalism, availability, and influence. Dr. Joe, as I got to know you, I realized that we are pretty much the same dude, just separated by around 30 years. You decided to take me on as a graduate student in a scenario where you had very little to gain, while also knowing that it would be a big time sink for you. Part of you doing that may have been based on friendship, but I know that the real reason is because you are a true educator. I

hold you in the absolute highest esteem, and consider you the biggest influence I've had. Dr. Joe, you're a great friend, a very cool dude, and a badass guitar player. I hope that, at some point in my life, I can help someone as much as you've helped me. Sincerely, thank you for everything.

TABLE OF CONTENTS

ACKNOWLEDGEMENTS ii

LIST OF TABLES x

LIST OF FIGURES xi

CHAPTER

I. INTRODUCTION AND ESSENTIAL BACKGROUND 1

1.1 Boundary Integral Methods 1
1.1.1 Green's Third Identity and the Green's Function 2
1.1.2 Continuity of the Density 5
1.1.3 Advantages of Boundary Integral Methods 5
1.1.4 Disadvantages/Challenges of Boundary Integral Methods . 6
1.2 Singular Integrals 8
1.2.1 The Cauchy Principal Value (Strongly Singular Integrals) . 9
1.2.2 The Hadamard Finite Part (Hypersingular Integrals) 10
1.2.3 Weakly Singular Integrals 11
1.2.4 Near Singular Integrals 12
1.2.5 Free-term Coefficient 13
1.3 Brief Overview of Contributions Provided by the Present Work . . 14
1.3.1 Contribution # 1: Smoothing of Near Hypersingular Integrals using an Elemental Distortion Technique 14
1.3.2 Contribution # 2: Efficient Approximation of Multivariate Weakly Singular Integrals by using Over-Regularization . . 15
1.3.3 Contribution # 3: High Order Interpolations with the Regularized Boundary Element Method in Three Dimensions . . 15

II. SMOOTHING OF NEAR-HYPERSINGULAR INTEGRALS USING AN ELEMENTAL DISTORTION TECHNIQUE 17

2.1 Abstract 17
2.2 Introduction 17
2.3 Smoothing of Integrals with Domain Transformations 19

2.3.1 The Duffy Transformation . . . 19
2.3.2 Further Smoothing with Nodal Offset . . . 22
2.3.3 Visual Improvement of the Integrability of a Near Singular Function . . . 26
2.4 Numerical Support of Concept . . . 28
2.4.1 Convergence and Efficiency Plots . . . 28
2.4.2 Three Primary Cases of Integration . . . 30
2.4.2.1 Source Point on Edge . . . 31
2.4.2.2 Source Point on Interior . . . 34
2.5 Numerical Example . . . 36
2.5.1 Convergence of Select Offsets . . . 37
2.6 Conclusion . . . 37

III. EFFICIENT APPROXIMATION OF MULTIVARIATE WEAKLY SINGULAR INTEGRALS BY USING OVER-REGULARIZATION . . . 41

3.1 Abstract . . . 41
3.2 Introduction . . . 41
3.3 Regularization . . . 43
3.3.1 Demonstration of Smoothing Effects . . . 44
3.3.2 Handling the Remainder Terms . . . 44
3.4 Order of Regularization Required . . . 47
3.5 Numerical Examples . . . 49
3.5.1 Straight-Sided Element Example . . . 49
3.5.2 Curved Element Example . . . 53
3.6 Conclusion . . . 58

IV. THE USE OF HIGH ORDER ELEMENTS IN THE BOUNDARY ELEMENT METHOD WITH REGULARIZATION . . . 60

4.1 Abstract . . . 60
4.2 Introduction . . . 60
4.2.1 The Case for a p-version BEM . . . 61
4.3 Modifying the BEM to Support High Order Elements with Regularization . . . 62
4.3.1 One-Term Regularization of Green's Third Identity . . . 64
4.3.2 Two-Term Regularization of Green's Third Identity . . . 65
4.3.3 Support of High Order Interpolations . . . 66
4.3.4 Controversy Surrounding the Simple Solutions Method . . . 67
4.4 Numerical Implementation . . . 70
4.4.1 Gaussian Quadrature . . . 70
4.4.2 Interpolation Functions . . . 71
4.4.3 Green's Third Identity . . . 72

4.4.4 Implementation of Simple Solutions 74
4.4.5 Linear System 77
4.5 Modelling of Geometries 77
4.5.1 Discretization of a Cube 77
4.5.2 Discretization of a Sphere 78
4.6 Numerical Examples 79
4.6.1 Steady State Heat Transfer on the Unit Cube: h-p Convergence (Example 1) 79
4.6.2 Steady State Heat Transfer on the Unit Cube: Increased Spatial Frequency (Example 2) 84
4.6.3 Steady State Heat Transfer on the Unit Sphere: Curved, General Surfaces (Example 3) 90
4.7 Conclusions 91

V. CONCLUSIONS 95

REFERENCES 96

LIST OF TABLES

1.1 A tabular reference for types of singularities existing in integrals. 9

2.1 Nodal locations for the Duffy transformation as shown in Figure 2.1. 19

2.2 Nodal locations for the transformation illustrated in Figure 2.5. 25

2.3 Nodal locations for the standard triangular subdomains. 32

3.1 Numerical results for the over-regularization of integral 3.6. 52

3.2 Numerical Results for the over-regularization of integral 3.9. 58

4.1 Results of interest for the unit sphere. 91

LIST OF FIGURES

1.1 Visualization of the geometry associated with Green's third identity. 4

1.2 Visualization of the exclusion region for singular integrals. 10

2.1 Transformation of a triangular domain to a Q4 element. 20

2.2 Visualization of the Duffy transformation for $f = 1/r$. 21

2.3 Visualization of the Duffy transformation for numerical quadrature. 23

2.4 Transformation of a triangular domain to a Q8 element. 24

2.5 Visualization of the Q8 transformation with nodal offset. 24

2.6 A comparison of a zero-nodal offset transformation versus an offset of $d = 0.2$. 27

2.7 Nodal offset efficiencies for integrand (2.7). 29

2.8 Standard triangular subdomains. 31

2.9 Nodal offset efficiencies for integrand (2.8). 33

2.10 A proposed triangular subdomain refinement. 34

2.11 Nodal offset efficiencies for integrand (2.8). 35

2.12 Nodal offset efficiencies for for integrand (2.11). 38

2.13 The effect of the nodal offset technique for EQ. (2.11). 39

3.1 A one-term regularization is applied to an integral. 45

3.2 Two-term and three-term regularizations are applied to an integral. 46

3.3 The effect of the regularized part of the integral trending downward in size. 48

3.4 The domain for the straight-sided element example (Q4 domain) is provided. 50

3.5 Visualization of the domain associated with the curved element example. . 54

3.6 A one-term regularization applied to integral 3.9. 56

3.7 Three and five-term regularizations applied to integral 3.9. 57

4.1 Polynomial refinement for the regularized integrand for $\phi(x) = e^x$. 69

4.2 Subdomains for numerical quadrature application. 71

4.3 Discretization of a cube (12 elements). 81

4.4 Discretization of a cube (300 elements). 82

4.5 h-p convergence on the unit cube. 83

4.6 Numerical approximations to ϕ across the cube edge $(x = 1, y, z = -1)$. . 85

4.7 Distribution of normalized errors for octic interpolations. 86

4.8 Distribution of normalized errors for decic interpolations. 87

4.9 Distribution of normalized errors for duodecic interpolations. 88

4.10 Fitting of numerical approximations (duodecic elements) to ϕ. 89

4.11 Discretization of a unit sphere (eight elements). 92

4.12 Numerical solution for ϕ across the sphere edge $(r = 1, \theta, z = 0)$. 93

CHAPTER I

INTRODUCTION AND ESSENTIAL BACKGROUND

1.1 Boundary Integral Methods

Boundary integral methods or boundary integral equation methods, sometimes referred to as the boundary element method(s) (BEM), are a class of numerical methods used to solve partial differential equation (PDE) problems in numerous areas of engineering and physics. The boundary element method is one particular subset of boundary integral methods. However, due to the popularity of this particular method, the terms "boundary integral methods" and "BEM" are used somewhat interchangeably. There are several different boundary integral methods, including the (direct) boundary element method [5], the indirect boundary element method [7], the method of functional equations, [50, 51] and the method of fundamental solutions [20], among others. The direct BEM often refers to a boundary integral method which places source points on the surface of the boundary to solve for the density and its flux, and integrates singular integrals that arise. The indirect BEM refers to a formulation which is similar to the direct BEM except that it solves for "ficticious" densities and fluxes which lack physical meaning but can be used to model physical quantities such as stress and displacement [7]. The method of functional equations places source points outside of the domain, resulting in near singular integrals [50,51]. The method of fundamental solutions is a meshless method which also places source points out-

side of the domain [20]. The symmetric Galerkin method is a Galerkin method which integrates over the source point coordinate in order to obtain a symmetric system matrix [89]. There are several other related methods to be found in the literature.

There are many different boundary integral methods, each with its own set of advantages and disadvantages. The material in this work is intended to support methods which can leverage direct integration with numerical quadrature, and also further the study of high order elements in boundary integral methods. However, the primary contribution in this work (Chapter IV) specifically targets the direct boundary element method.

Boundary integral methods have several notable advantages, but one unique and powerful advantage is that they offer the ability to reduce the dimensionality of a problem by only requiring integration over the surface. In other words, a three-dimensional solution can be obtained from a two-dimensional integral, and a two-dimensional solution can be obtained from a one-dimensional integral. This also implies that for a three-dimensional problem, a two-dimensional mesh is required, and for a two-dimensional problem, a one-dimensional mesh is required. This can be observed from Green's third identity [46].

1.1.1 Green's Third Identity and the Green's Function

Green's third identity for the three dimensional Laplace's equation is shown in EQ. (1.1), which serves as the basis for the boundary integral methods discussed in this work,

$$\underbrace{\phi(\mathbf{p})}_{\text{Three-dimensional field}} = \underbrace{\iint_{\mathrm{S}} \left(\psi(\mathbf{p},\mathbf{Q}) \frac{\mathrm{d}\,\phi(\mathbf{Q})}{\mathrm{d}\hat{n}(\mathbf{Q})} - \phi(\mathbf{Q}) \frac{\mathrm{d}\psi(\mathbf{p},\mathbf{Q})}{\mathrm{d}\hat{n}(\mathbf{Q})} \right) \mathrm{dS}(\mathbf{Q})}_{\text{Two-dimensional integral}}, \tag{1.1}$$

where

- $\mathbf{p}$ is referred to as the source point. The coordinate $\mathbf{p}$ refers to any three-dimensional location. This point is designated by the Cartesian coordinates (X_p, Y_p, Z_p).
- $\mathbf{Q}$ is referred to as the field point(s). The coordinate $\mathbf{Q}$ refers to locations on the surface of integration. Points on this surface are designated by the Cartesian coordinates (X_Q, Y_Q, Z_Q).
- $\phi(\mathbf{p})$ represents a potential function in three dimensions. This function is a scalar field, represented as a function of the source point coordinate ($\mathbf{p}$).
- $\phi(\mathbf{Q})$ represents the surface density. That is, the portion of the potential function that coincides with the surface $(\mathbf{Q})$. Note that $\phi(\mathbf{Q})$ is a subset of $\phi(\mathbf{p})$.
- $\frac{\mathrm{d}\,\phi(\mathbf{Q})}{\mathrm{d}\hat{n}(\mathbf{Q})}$ refers to the normal derivative, which is $\vec{\nabla}\phi \cdot \hat{n}(\mathbf{Q})$.
- $\psi(\mathbf{p}, \mathbf{Q})$ is the Green's function in three dimensions also known as the fundamental solution. This term is a scalar field, which is a function of geometry. It is useful to note that ψ is $1/4\pi r$, where r is the straight line distance between $\mathbf{p}$ and $\mathbf{Q}$. The Green's function and its derivative are referred to as kernels.
- $\frac{\mathrm{d}\,\psi(\mathbf{Q})}{\mathrm{d}\hat{n}(\mathbf{Q})}$ refers to the normal derivative, which is $\vec{\nabla}\psi \cdot \hat{n}(\mathbf{Q})$.

The point $\mathbf{p}$ is used to denote a point which can be located *any*where in space. If $\mathbf{p}$ is located on the surface, it is commonly denoted with a capital letter ($\mathbf{P}$), and if it is elsewhere, it is denoted as $\mathbf{p}$ (see Figure 1.1). The point $\mathbf{P}$ indicates the possibility of singular integrals. The source point $\mathbf{Q}$, is used to denote only locations on the surface. To evaluate the function $\phi(\mathbf{p})$ at some point inside of the domain, $\mathbf{p}$, a value can be obtained by (numerically) integrating over the surface of the domain (which again, is denoted by $\mathbf{Q}$). EQ. (1.1) demonstrates that by solving a two-dimensional surface integral (which can be discretized and solved numerically), a solution across three dimensions can be obtained. Numerical implementation of the boundary form of this equation is provided in Chapter IV. The reader is also directed to [65] for a derivation of EQ. (1.1).

For the Laplacian operator,

$$\nabla^2\phi = 0. \tag{1.2}$$

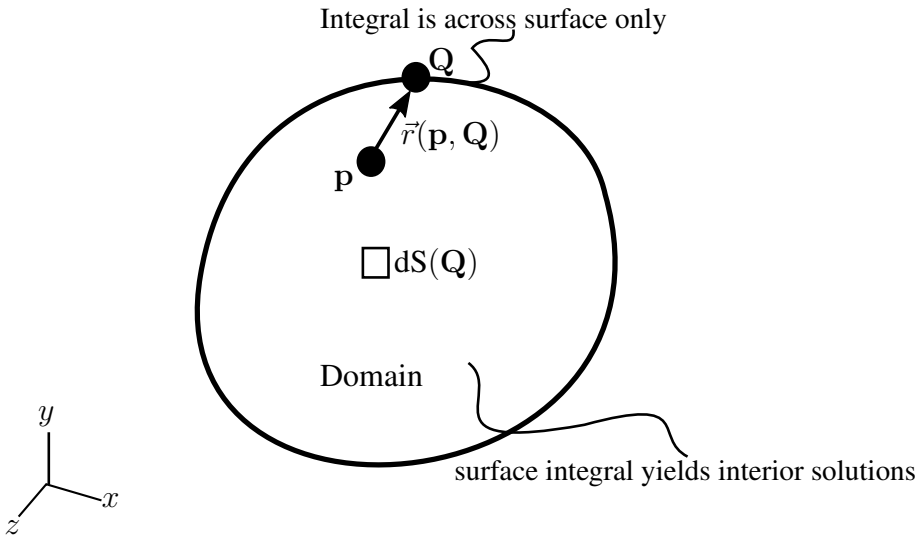

Figure 1.1

Visualization of the geometry associated with Green's third identity, as shown in EQ. (1.1).

the Green's function in three dimensions, often referred to as the free-space Green's function, is [46],

$$\psi(\mathbf{p}, \mathbf{Q}) = \frac{1}{4\pi r(\mathbf{p}, \mathbf{Q})}. \tag{1.3}$$

The distance between the points **p** and **Q**, $r(\mathbf{p}, \mathbf{Q})$ is,

$$r(\mathbf{p}, \mathbf{Q}) = \sqrt{((X_p - X_Q)^2 + (Y_p - Y_Q)^2 + (Z_p - Z_Q)^2}. \tag{1.4}$$

Note that the Green's function is unique to the operator, but is generally a function of $1/r$. The Green's function is also known as the fundamental solution, which indicates that it is a solution to,

$$\nabla^2 \psi = -\mathscr{D}(\mathbf{P}, \mathbf{Q}), \tag{1.5}$$

where $\mathscr{D}(\mathbf{P}, \mathbf{Q})$ is the Dirac delta generalized function, representing a point charge. It is also referred to as a unit impulse, because it exhibits the properties,

$$\begin{aligned} \mathscr{D}(\mathbf{p}, \mathbf{Q}) &= 0 \quad \text{for} \quad \mathbf{p} \neq \mathbf{Q} \\ \int_{\Omega} \mathscr{D}(\mathbf{p}, \mathbf{Q}) \mathrm{d}\Omega(\mathbf{Q}) &= 1 \quad \text{for} \quad \mathbf{p} \in \Omega(\mathbf{Q}). \end{aligned} \tag{1.6}$$

1.1.2 Continuity of the Density

It is useful to state that in order for the surface form of the integral in EQ. (1.1) to exist, ϕ must be Hölder continuous [60]. The Hölder condition states that if f is Hölder continuous, there exist some constants C and α that satisfy the condition [64],

$$|f(u_2, v_2) - f(u_1, v_1)| \leq C\left(|u_2 - u_1|^{\alpha} + |v_2 - v_1|^{\alpha}\right), \tag{1.7}$$

where u and v represent general surface coordinates. Functions are often stated to be $C^{1,\alpha}$, which states that functions are Hölder continuous in the first derivative. A function that was $C^{2,\alpha}$ would be Hölder continuous in the second derivative. The Hölder condition can be thought of as the weakest theoretical statement of continuity for a singular integral to be finite.

1.1.3 Advantages of Boundary Integral Methods

The computational efficiency gained by this reduction provides a possible advantage over many popular numerical methods, such as the finite element method, the finite volume method, and the finite difference method. Another powerful advantage exists for external problems requiring boundary conditions at infinity, such as acoustics [55] or flow over an

airfoil [67]. The integral formulation of these problems directly handles boundary conditions at infinity. For example, the airfoil problem only requires a surface discretization of the wing. A domain method would require a large discretization of the volume and can only approximate remote boundary conditions. In short, the attraction of boundary integral methods is that degrees of freedom (DOF) are of size $\mathscr{O}(N^2)$, which is favorable over domain techniques which require DOF of size $\mathscr{O}(N^3)$. A reduction in DOF results in a smaller linear system. The reduction in dimensionality occurs because a three-dimensional solution is obtainable from a two dimensional integral, and a two-dimensional solution is obtainable from a one-dimensional integral.

1.1.4 Disadvantages/Challenges of Boundary Integral Methods

This reduction in DOF is not free, however. While computational efficiency is gained, some mathematical difficulties arise. Specifically, the primary mathematical challenge of boundary integral methods is that of computing singular integrals. Boundary integral methods have been criticized for being mathematically complex in comparison with other popular methods [7], and this is largely due to the singular integral. Singular/near singular integrals represent a large portion of study (both current and previous) in boundary integral methods, and have been the primary drawback of the BEM since its early development [54]. Many BEM formulations require closed form integration techniques to evaluate singular integrals, and this becomes a significant, often unfeasible challenge when interpolation order increases. Chapter IV will offer a regularization method that sidesteps many

of the challenges associated with singular integrals in the BEM, specifically in the direct BEM.

The primary limitation of the boundary integral methods is a requirement for a free-space Green's function for the differential operator governing the problem of interest. If a linear problem lacks a known Green's function, approximate Green's functions are one way to handle this [9]. Nonlinear problems also lack a closed form Green's function. One clear example are turbulent, nonlinear flow problems, which are governed by the Navier-Stokes equations. Another example may be high-deformation, nonlinear elasticity, where the assumption of small strain is not made (for example, problems characterized by Green-St. Venant strain [58]).

Additionally, the reduction in system size in boundary integral methods is partially offset by the fact that boundary integral methods typically generate a dense system matrix, as opposed to the FEM which has a larger, but very sparse, symmetrical system matrix.

Other disadvantages include nonlinear problems and thin-body problems [5, 7]. Thin-body problems give rise to near singular integrals, due to the large surface-to-volume ratio, and this often results in inaccuracies in numerical integration in the absence of an effective quadrature technique. However, the methods discussed in Chapter II may improve near singular integration issues in this context.

Problems with sharp gradients and/or rapid spatial variation may also be an issue for many BEM codes. Most BEM codes use quadratic interpolations, and are limited to h-refinement (i.e. refining the mesh). However, Chapter IV will demonstrate that the BEM

can support hp-refinement (i.e. increasing the order of interpolation functions and refining the mesh), and this will show significant improvement.

With minor exceptions, there appear to be few problems that the BEM cannot handle as efficiently as the FEM [5, 7].

1.2 Singular Integrals

It is observed that as $\mathbf{p}$ approaches $\mathbf{Q}$, the Green's function, EQ. (1.3), will become unbounded giving rise to a singularity. Because the Green's function is a function of distance, it will vary rapidly as the singularity is approached. Handling this may require a mathematical reformulation or extra modeling fidelity.

As previously mentioned, singular integrals represent a large portion of work in boundary integral methods. Understanding the differences between different types of singularities is essential in the analysis of boundary integral methods, as each type of singularity will require a specific approach. For simplicity, concepts will be demonstrated here with one-dimensional integrals. Singular integrals (denoted here generally as I) may be expressed in a form resembling (one-dimensional form shown here for simplicity) [21],

$$I = \int_a^b \frac{f(x)}{(x - x_0)^{n+1}} \mathrm{d}x, \ -\infty < a < x_0 < b < \infty, \quad n = 1, 2, 3... \tag{1.8}$$

Without modification, these integrals often diverge and must be interpreted as improper integrals. If the integral is weakly singular, the integral may be evaluated with numerical quadrature. Higher order singularities require special interpretation. EQ. (1.8) shows that as x approaches x_0 the integrand will approach a division by zero near the singularity at $x = x_0$. A quick reference for singularities is provided in Table 1.1.

Table 1.1

A tabular reference for types of singularities existing in integrals. The strength of the singularity depends on the dimensionality of the integral.

Singularity Type	One-Dimensional	Two-Dimensional	Interpretation
Weakly singular	$f\left(\ln(r)\right)$	$f\left(1/r\right)$	Ordinary
Strongly Singular	$f\left(1/r\right)$	$f\left(1/r^2\right)$	Cauchy Principal Value
Hypersingular	$f\left(1/r^2\right)$	$f\left(1/r^3\right)$	Hadamard Finite Part

1.2.1 The Cauchy Principal Value (Strongly Singular Integrals)

In a three-dimensional problem (involving a two-dimensional integral), an integral is considered strongly singular if the singularity has an order of $n = 1$, $(1/r^2)$, and in a two-dimensional problem (involving a one-dimensional integral), an integral is considered strongly singular if the singularity has an order $n = 0$, $(1/r)$, as shown in EQ. (1.9) [74]. The strongly singular integral does not exist in the sense of the Riemann sum, and must be interpreted as a Cauchy principal value (CPV). Unlike the weakly singular integral, a strongly singular integral requires special interpretation involving a limit [30, 48]. This process defines an exclusion region around the singularity bounded by a radius of size ϵ as shown in Figure 1.2. A specific form of the strongly singular integral for two-dimensional problems on a flat surface would be (shown in one dimension for simplicity),

$$CPV[I] = \overset{\text{CPV}}{\int_a^b} \frac{f(x)}{(x-x_0)}\mathrm{d}x = \lim_{\epsilon\to 0}\left[\int_a^{x_0-\epsilon} \frac{f(x)}{(x-x_0)}\mathrm{d}x + \int_{x_0+\epsilon}^b \frac{f(x)}{(x-x_0)}\mathrm{d}x\right]. \quad (1.9)$$

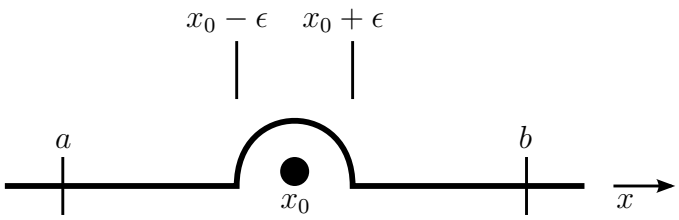

Figure 1.2

The singularity is isolated by an exclusion region of radius ϵ during the limiting process of the Cauchy principal value and Hadamard finite part interpretations.

The interpretation given to the limit, if it exists, is known as the Cauchy principal value. The superscript CPV in EQ. (1.9) denotes the requirement of the Cauchy principal value to interpret the integral.

1.2.2 The Hadamard Finite Part (Hypersingular Integrals)

In three dimensions (involving two-dimensional integrals) an integral is considered hypersingular if it contains a singularity of order $n = 2$, $(1/r^3)$, and in two dimensions (involving a one-dimensional integral), an integral is considered hypersingular if it contains a singularity of order $n = 1$, $(1/r^2)$, as shown in EQ. (1.10) [74]. The hypersingular integral must also be interpreted in a special sense. Much like the CPV, the Hadamard finite part (HFP) requires special interpretation with a limiting process, as it is the derivative with respect to x_0 of the CPV (the Leibniz integral rule is used here).

$$HFP[I] = \overset{\text{HFP}}{\int_a^b} \frac{f(x)}{(x-x_0)^2}\mathrm{d}x = \lim_{\epsilon\to 0}\left[\int_a^{x_0-\epsilon} \frac{f(x)}{(x-x_0)^2}\mathrm{d}x + \int_{x_0+\epsilon}^b \frac{f(x)}{(x-x_0)^2}\mathrm{d}x - \frac{2\,f(x_0)}{\epsilon}\right] \tag{1.10}$$

The interpretation given to the limit, if it exists, is known as the Hadamard Finite Part (HFP). The superscript HFP in EQ. (1.10) denotes the requirement of the Hadamard finite part to interpret the integral.

1.2.3 Weakly Singular Integrals

In three-dimensional problems (involving two-dimensional boundary integrals), an integral is considered weakly singular if it has an integrable singularity of order $n = 0$, $(1/r)$, and in a two-dimensional problem (involving a one-dimensional integral), an integral is considered weakly singular if the kernel contains $\ln(r)$. *While weakly singular integrals have a point at which the kernel becomes undefined, they do exist in the ordinary sense*, and may be evaluated with numerical quadrature. In order words, the integrals do exist in the sense of a Riemann sum. A weakly singular integral has a point where it becomes undefined, but the integral converges to a finite value.

Gaussian quadrature is a technique that numerically evaluates an integral by effectively approximating the integrand as a polynomial. The result is that the integral can be represented by a summation of the function evaluated at locations referred to as "Gauss points" and their associated weights,

$$\int f(x)\mathrm{d}x \approx \sum_{i=1}^{\mathrm{NGP}} W_i\, f(x_i) \tag{1.11}$$

where NGP is the number of Gauss points, x_i are the locations of the Gauss points, and W_i are the weights associated with those Gauss points. The locations x_i are obtained from roots of the Gauss-Legendre polynomial. For a basic review on Gaussian quadrature, the reader is directed to [8].

Due to the rapidly varying nature around x_0 (as represented in EQ. (1.8)), evaluating a weakly singular integral with numerical quadrature is usually done by way of a domain or coordinate transformation. Many popular approaches for evaluating a weakly singular integral with quadrature are based on the "Duffy transformation" [19], which effectively smooths the function by performing a domain transformation. While there are more efficient methods, the accuracy of the Duffy transformation is primarily limited by the number of Gauss points. For context, this work shows results of the Duffy transformation obtaining three significant digits with a 100 point rule, and 13 significant digits with a 900 point rule. However, the success of the Duffy method does depend on the placement of **p** and **Q**. The Duffy transformation is discussed in detail in Section 2.3.1.

For quadrature-related studies in the context boundary integrals, the reader is directed to [19,24–26,35,39–43,56,84,86,87,93,95,97–99], although this is not an exhaustive list. Typically, once an integral is in a weakly singular form, direct numerical integration can be performed. Chapter III addresses the problem of approximating weakly singular integrals.

1.2.4 Near Singular Integrals

Near singular integrals occur when the source point of a Green's function is offset from the surface by some small distance, D. This results in an integral in a form resembling,

$$I = \int_a^b \frac{f(x)}{\left(\sqrt{(x-x_0)^2 + D^2}\right)^{n+1}} \mathrm{d}x, \quad -\infty < a < x_0 < b < \infty, \quad n = 1, 2, 3... \quad (1.12)$$

Near singular integrals are finite but may be difficult to integrate numerically, depending on how small the offset, D, is, and what the order of near singularity is. Depending on the value of n, an integral may be near weakly singular, near strongly singular, or near

hypersingular. These classifications are the same as shown in Table 1.1, with the inclusion of the offset D. While near singular integrals are regularly studied, numerical quadrature for these integrals is an ongoing area of research. Near singular integrals often appear in thin body problems [7], and in the method of functional equations [50, 51]. Guidelines for choosing D is also an area of research [45], particularly in literature surrounding the method of functional equations [10]. Chapter II addresses the problem of efficient integration of near singular integrals.

1.2.5 Free-term Coefficient

Depending on the placement of **p**, the term attached to the free-term coefficient in EQ. (1.1) will vary. This falls from the integral of the flux of the Green's function attached to ϕ during the derivation of Green's third identity. For the interior form, the free-term coefficient is 1, as shown in EQ. (1.1). For the boundary form, the free-term coefficient is ½ for smooth points. For the exterior form, the free-term coefficient is 0. All three forms are now provided.

The interior form (**p** inside of the domain, but not on the boundary) is,

$$\phi(\mathbf{p}) = \iint_{\mathrm{S}} \left(\psi(\mathbf{p},\mathbf{Q}) \frac{\mathrm{d}\,\phi(\mathbf{Q})}{\mathrm{d}\hat{n}(\mathbf{Q})} - \phi(\mathbf{Q}) \frac{\mathrm{d}\psi(\mathbf{p},\mathbf{Q})}{\mathrm{d}\hat{n}(\mathbf{Q})} \right) \mathrm{dS}(\mathbf{Q}). \tag{1.13}$$

The boundary form (**P** on the boundary) is,

$$\frac{1}{2}\phi(\mathbf{P}) = \iint_{\mathrm{S}} \left(\psi(\mathbf{P},\mathbf{Q}) \frac{\mathrm{d}\,\phi(\mathbf{Q})}{\mathrm{d}\hat{n}(\mathbf{Q})} \right) \mathrm{dS}(\mathbf{Q}) - \overset{\mathrm{CPV}}{\iint_{\mathrm{S}}} \left(\phi(\mathbf{Q}) \frac{\mathrm{d}\psi(\mathbf{P},\mathbf{Q})}{\mathrm{d}\hat{n}(\mathbf{Q})} \right) \mathrm{dS}(\mathbf{Q}). \tag{1.14}$$

The exterior form (**p** outside of the domain) is,

$$0 = \iint_{\mathrm{S}} \left(\psi(\mathbf{p},\mathbf{Q}) \frac{\mathrm{d}\,\phi(\mathbf{Q})}{\mathrm{d}\hat{n}(\mathbf{Q})} - \phi(\mathbf{Q}) \frac{\mathrm{d}\psi(\mathbf{p},\mathbf{Q})}{\mathrm{d}\hat{n}(\mathbf{Q})} \right) \mathrm{dS}(\mathbf{Q}). \tag{1.15}$$

1.3 Brief Overview of Contributions Provided by the Present Work

The present work aims to provide three contributions to boundary integral methods literature. The three contributions are as follows.

1.3.1 Contribution # 1: Smoothing of Near Hypersingular Integrals using an Elemental Distortion Technique

Boundary integral methods exhibit near singular integrals in a number of cases. The primary cases are for thin-body problems [5, 7], which exhibit a large surface-to-volume ratio, and the method of functional equations [50, 51]. The method of functional equations easily supports high order elements and can be seen as a way to avoid the problem of singular integrals by formulating a problem with near singular integrals. Near singular problems may exhibit near weakly singular, near strongly singular, and near hypersingular integrals. The near hypersingular integral is the most difficult of these three to integrate, hence it will receive focus here.

For these reasons, a more efficient scheme for direct integration of near hypersingular singular integrals is desired. Presently, a number of integral transformation techniques exist which produce effective quadrature schemes for different cases and classes of near singular integrals [24–26, 35, 39–43, 87, 93, 95, 97–99]. While these works showed success, improvement in numerical quadrature is always desired.

This work includes a new approach for developing quadrature schemes for near hypersingular integrals. By performing a domain transformation with quadratic elements, a parameter of distortion is introduced which can be varied to obtain a more efficient quadra-

ture pattern than standard techniques. It is shown that the number of points required for near hypersingular integrals may be reduced up to 75% using this new technique.

1.3.2 Contribution # 2: Efficient Approximation of Multivariate Weakly Singular Integrals by using Over-Regularization

Boundary integral methods, especially ones using regularization (see Chapters III,IV), often rely on efficient integration of the weakly singular integral. There are a number of techniques for integrating the weakly singular integral [19, 66, 84, 86, 88]. The literature shows few quadrature techniques that are based in regularization, which may offer a greater reduction in quadrature points than other methods. This work offers a technique, based on regularization [4, 13, 71–74, 78, 81, 83, 85, 92, 94], which allows for a weakly singular integral to be decomposed into two parts: a regular part and a remainder. The regular part is amenable to direct application of a quadrature rule, as the integrand has been smoothed, and the singularity is reduced. The remainder is often in a form which is convenient for closed form integration. This decomposition allows for a hybrid numerical-analytical approach which simplifies the problem of the weakly singular integral, and increases computational efficiency. The method does not require a domain transformation, although it can support one if desired.

1.3.3 Contribution # 3: High Order Interpolations with the Regularized Boundary Element Method in Three Dimensions

Most BEM codes rely on closed-form integration to handle the problem of the singular integral. Because of this, most works in the BEM only use quadratic interpolations to model the surface density, as closed form integration of higher-order interpolations is

difficult. Closed form integration is often unfeasible, largely due to the variation of the Jacobian. Presently, there are only a number of works which have attempted high order modeling in BEM [4, 34, 71–73], and of these works, only Richardson and Arjunon's conference paper in 2009 [72] addressed a three-dimensional problem.

There exist regularization techniques which both completely avoid the problem of singular integrals while also allowing for the BEM to directly support high order interpolations. Regularization allows for the reduction of both strongly singular and hypersingular integrals to be reduced to a weakly singular form including use of the simple solutions method [78]. The weakly singular form can then be directly evaluated with numerical quadrature. Without using regularization, one must rely on analytic formulæ to evaluate the strongly singular and hypersingular integrals in closed form, which prevents use of high order interpolations.

Chapter IV demonstrates that a three-dimensional BEM can be regularized with the simple solutions technique, thus supporting use of high order interpolations while only requiring numerical quadrature. Additionally, a case is made for a p-version BEM by demonstrating the increase in computational efficiency through p-refinement, and demonstrating the ability for high order elements to capture densities with significant spatial variation.

CHAPTER II

SMOOTHING OF NEAR-HYPERSINGULAR INTEGRALS USING AN ELEMENTAL DISTORTION TECHNIQUE

2.1 Abstract

The present work offers a new transformation scheme, based on the Duffy transformation, which leverages quadratic shape functions to introduce a degree-of-freedom associated with nodal offset. By optimizing this offset variable, an elemental distortion occurs which improves the integrability of the integrand in the transformed domain. General approaches and a practical example representative of the method of functional equations across a triangular element are included.

2.2 Introduction

A wide array of physics problems are governed by partial differential equations (PDEs) which can be reformulated as a set of integral equations. Problems in potential theory [46] and boundary element methods [7] use the free-space Green's function [23] to perform this reformulation in such a way that allows the dimensionality of the problem to be reduced by one. The use of the Green's function will often result in a singular, or near singular integral. Singular integrals often appear in a form resembling [21],

$$CPV[I] = \overset{\text{CPV}}{\int_a^b} \frac{f(x)}{(x-x_0)}\mathrm{d}x = \lim_{\epsilon\to 0}\left[\int_a^{x_0-\epsilon} \frac{f(x)}{(x-x_0)}\mathrm{d}x + \int_{x_0+\epsilon}^b \frac{f(x)}{(x-x_0)}\mathrm{d}x\right].$$
$$HFP[I] = \overset{\text{HFP}}{\int_a^b} \frac{f(x)}{(x-x_0)^2}\mathrm{d}x = \lim_{\epsilon\to 0}\left[\int_a^{x_0-\epsilon} \frac{f(x)}{(x-x_0)^2}\mathrm{d}x + \int_{x_0+\epsilon}^b \frac{f(x)}{(x-x_0)^2}\mathrm{d}x - \frac{2\,f(x_0)}{\epsilon}\right] \tag{2.1}$$

where CPV and HFP represent the Cauchy principal value and Hadamard finite part interpretations, respectively. Depending on the order of the singularity, the integral may be evaluated directly with quadrature, or it may require special mathematical interpretation. Weakly singular and near singular integrals may be evaluated with quadrature while singular integrals are interpreted by taking a limit as the radius around the singularity approaches zero as shown in EQ. (2.1). Interpreting finite values for special integrals was first performed by Hadamard [30].

This particular study addresses the numerical integration of near hypersingular integrals. Near hypersingular integrals often arise in thin body problems [52, 53, 93], the method of fundamental solutions [10], and the method of functional equations [50, 51]. Several effective transformations for near singular integrals have been posed and successfully applied [24–26,35,39–43,87,93,95,97–99], as well as direct quadrature methods [56]. Many of these outperform the standard Duffy transformation [19], which serves as a basis for the concept presented. A new type of transformation which results in efficient quadrature schemes in the context of near singular integrals is also presented.

2.3 Smoothing of Integrals with Domain Transformations

2.3.1 The Duffy Transformation

When using quadrature to evaluate a rapidly varying integrand, one common technique which can be employed is that of a domain transformation. The success of such a domain transformation is that, transforming a function from one set of coordinates to another leads to an integrand more suitable for approximate integration. An example of this concept appears to be first presented by Duffy in [19], and is often referred to as the Duffy transformation. One has the option of integrating the smoothed function in the new space, or transforming back to the original space to store a new quadrature pattern. An excellent candidate for the Duffy transformation is the weakly singular kernel in three dimensions, $1/r$. To illustrate this type of transformation, a diagram is provided in Figure 2.1. For context, linear planar elements such as the T3 and Q4 elements used in two-dimensional finite element methods are used.

Table 2.1

Nodal locations for the transformation from a triangular element to a Q4 element, as shown in Figure 2.1.

	x	y	ξ	η
Node 1	0	1	-1	1
Node 2	0	0	-1	-1
Node 3	1	0	1	-1
Node 4	0	1	1	1

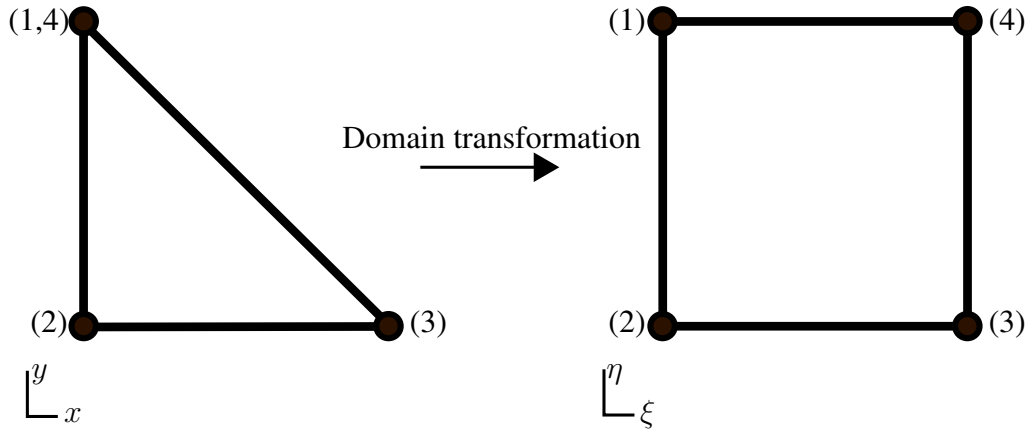

Figure 2.1

Transformation of a triangular domain (left) to a Q4 element (right).

It should be noted that the locations given for the triangular domain are often associated with the T3 element, and will be referred to as the "standard triangular domain" throughout. One simple way to perform this transformation is by using standard shape functions. This is performed by assuming that the triangular domain is a Q4 domain with coincident nodes 1 and 4. For reference, the Q4 shape functions are provided as [100],

$$\begin{aligned} N_1 =& \frac{1}{4}(1-\xi)(1-\eta) \\ N_2 =& \frac{1}{4}(1+\xi)(1-\eta) \\ N_3 =& \frac{1}{4}(1+\xi)(1+\eta) \\ N_4 =& \frac{1}{4}(1-\xi)(1+\eta). \end{aligned} \tag{2.2}$$

Using the transformation outlined above, one may consider the behavior of the function f,

$$f = \frac{1}{\sqrt{x^2+(y-1)^2}} = \frac{1}{r} \tag{2.3}$$

as (x, y) approaches nodes (1,4) in the triangular (x, y) domain. By transforming f to the coordinate system (ξ,η), the weak singularity can be "stretched" and "smoothed" in such a way that is favorable for direct application of quadrature. This effect can be observed in Figure 2.2.

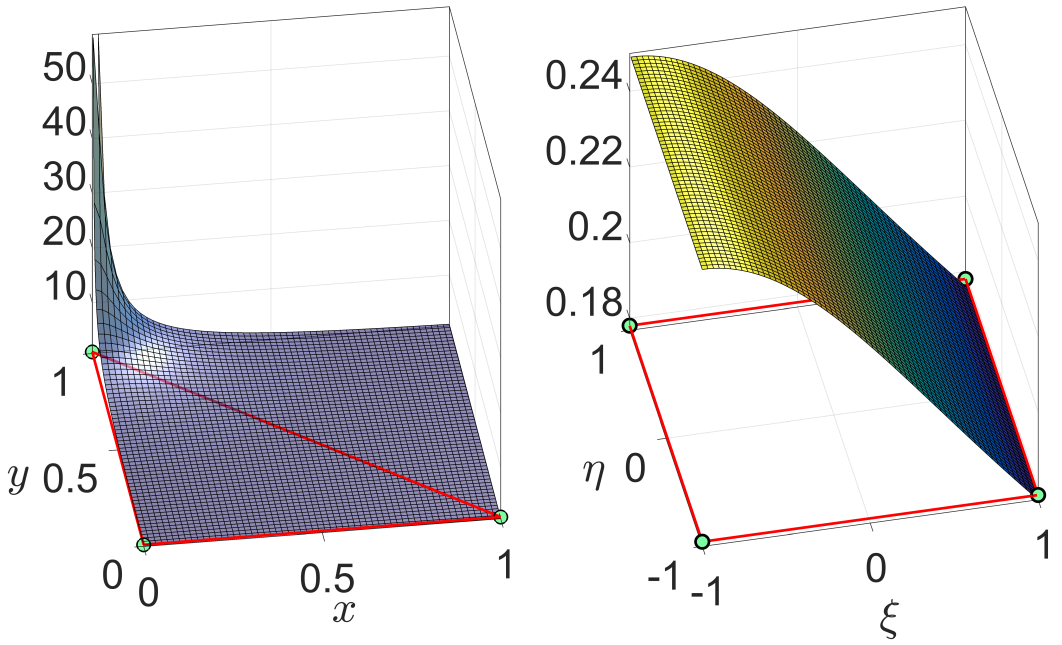

Figure 2.2

Transformation of $f = 1/r$ from a triangular domain (left) to a Q4 domain (right).

Figure 2.2 shows an example of the Duffy transformation. While the integrand is steeply varying in the original space, the transformation to a new set of coordinates results in a Jacobian of transformation that effectively smooths the integrand. It should be noted that due to the smoothness of the integrand in the Q4 domain, standard quadrature patterns can be applied. Assuming that one seeks to integrate in the triangular domain, a

quadrature pattern can be applied in the Q4 domain, and transformed back to the triangular domain. A visualization of this pattern is given in Figure 2.3.

Figure 2.3 shows that quadrature points are stacked horizontally as the singularity is approached. A specifically tailored quadrature pattern such as this will outperform the direct application of a general pattern in terms of both accuracy and efficiency. The location of points in Figure 2.3 suggest that improved placement of points in the radial direction may offer an increase in efficiency and accuracy.

2.3.2 Further Smoothing with Nodal Offset

It has been observed that the quadrature shown in Figure 2.3 shows little improvement in the radial direction (directly toward the singularity from any point on the element). In response, a concept is now introduced and investigated. The use of a higher order model of the domain will provide nodes which can be transformed in such a way that the resulting quadrature locations are both horizontally and radially condensed. The question arises as to whether this condensing of quadrature points makes a near singular function more integrable in the natural coordinate system (ξ, η). To perform this transformation, a triangular domain is treated as a Q8 element, as opposed to a Q4. However, the locations of the nodes in the triangular domain are offset by a constant that will be hence referred to as d. The modified nodal locations are given in Table 2.2. Additionally, the Q8 shape functions are provided in EQ. (2.4) [100].

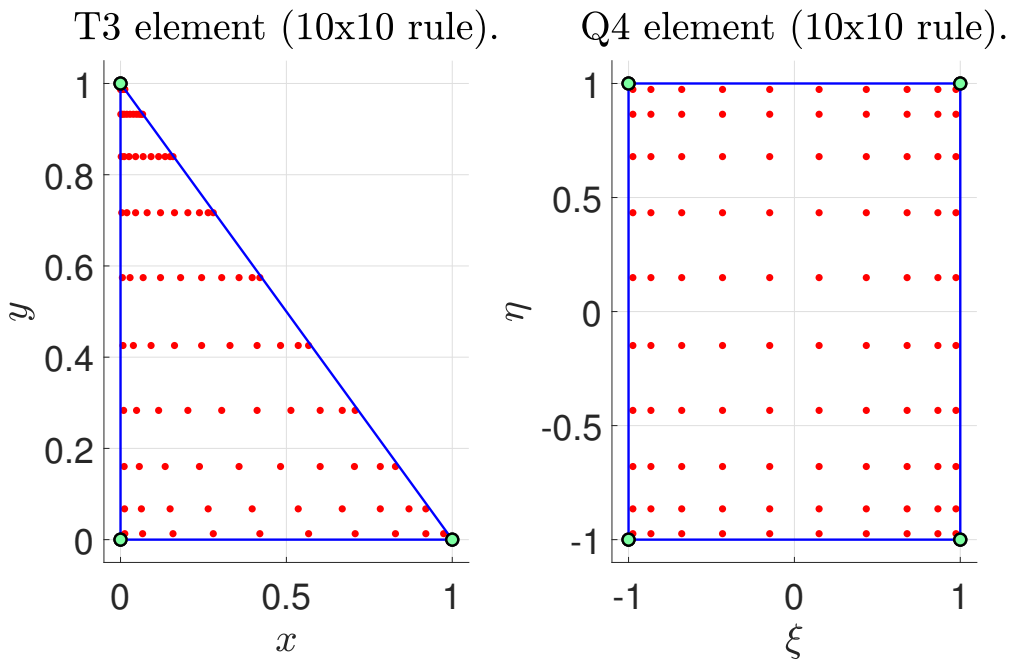

Figure 2.3

Standard Gauss-Legendre quadrature is applied to the Q4 domain (right) and then transformed back to the triangular domain (left) to obtain a quadrature pattern that is well suited for the direct integration of weakly singular integrals.

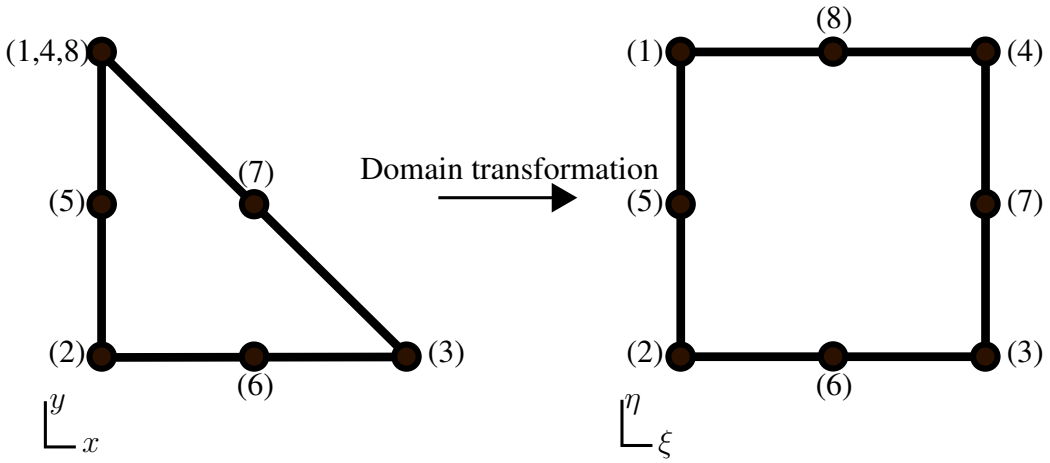

Figure 2.4

Transformation of a triangular domain (left) to a Q8 element (right).

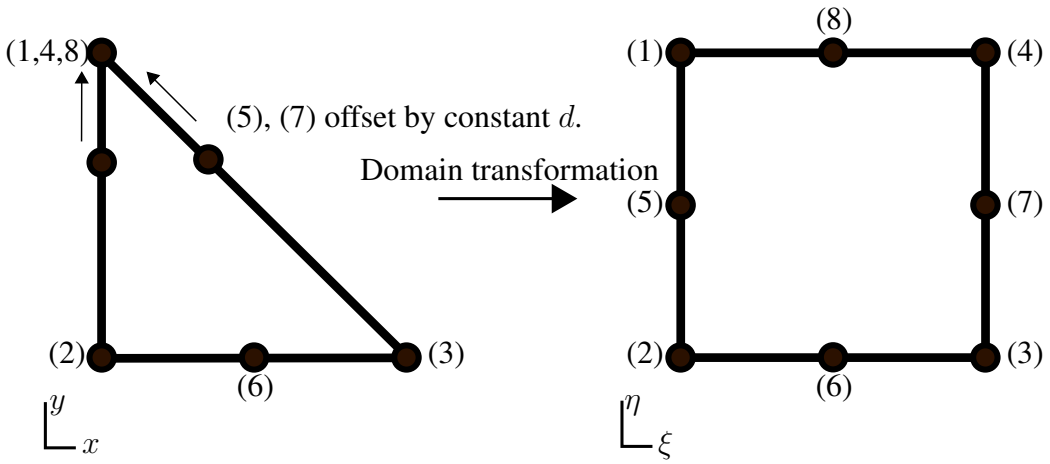

Figure 2.5

Transformation of a triangular domain (left) to a Q8 element (right) using a nodal offset distance, d.

Table 2.2

Nodal locations for the nodal offset transformation technique as illustrated in Figure 2.5.

Note the inclusion of the nodal offset variable, d.

	x	y	ξ	η
Node 1	0	1	-1	1
Node 2	0	0	-1	-1
Node 3	1	0	1	-1
Node 4	0	1	1	1
Node 5	0	0.5+d	-1	0
Node 6	0.5	0	0	-1
Node 7	0.5-d	0.5+d	1	0
Node 8	0	1	0	1

$$
\begin{aligned}
N_1 =& \frac{1}{4}(\xi-1)\ (\eta+1)\ (\xi-\eta+1)\\
N_2 =& -\frac{1}{4}(\xi-1)\ (\eta-1)\ (\eta+\xi+1)\\
N_3 =& \frac{1}{4}(\xi+1)\ (\eta-1)\ (\eta-\xi+1)\\
N_4 =& \frac{1}{4}(\xi+1)\ (\eta+1)\ (\eta+\xi-1)\\
N_5 =& \frac{1}{2}\left(\eta^2-1\right)\ (\xi-1)\\
N_6 =& \frac{1}{2}\left(\xi^2-1\right)\ (\eta-1)\\
N_7 =& -\frac{1}{2}\left(\eta^2-1\right)\ (\xi+1)\\
N_8 =& -\frac{1}{2}\left(\xi^2-1\right)\ (\eta+1)
\end{aligned}
\tag{2.4}
$$

2.3.3 Visual Improvement of the Integrability of a Near Singular Function

As an introductory example, the near hypersingular function

$$
f = \frac{1}{\left(x^2+(y-1)^2+(0.1)^2\right)^{3/2}} \tag{2.5}
$$

is integrated over the standard triangular domain. This is a representation of a near hypersingular function for a point $\mathbf{p}$ located ten percent of the characteristic element length from the surface. Figure 2.6 shows a standard Duffy transformation (left) versus the proposed transformation (right).

Figure 2.6 shows that performing a domain transformation by moving nodes closer to the near singularity offers the ability for further smoothing beyond the concept of a Duffy transformation. The question which remains is whether there is an optimal nodal offset distance, d.

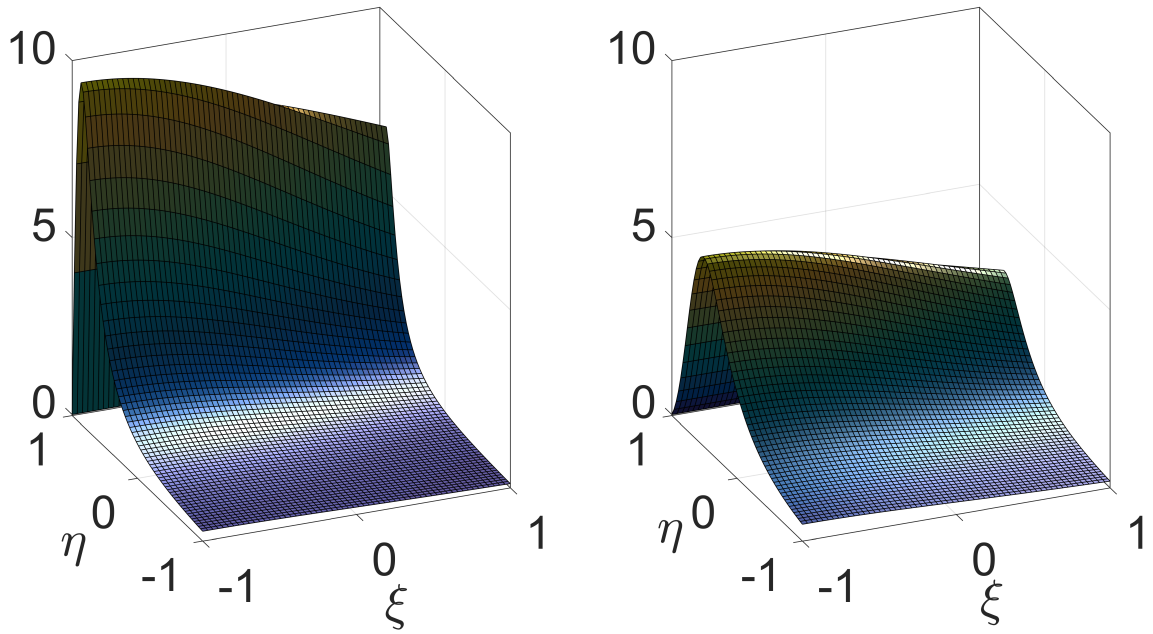

Figure 2.6

A comparison of a zero-nodal offset transformation (left) versus an arbitrary nodal offset of $d = 0.2$ (right) for f in EQ. (2.5).

2.4 Numerical Support of Concept

2.4.1 Convergence and Efficiency Plots

Figure 2.6 demonstrates that the proposed concept can offer further smoothing. Nodal offsets between zero and the quarter point [6,37] are investigated for the near hypersingular integral, f,

$$f(x,y) = \frac{1}{\left(x^2 + (y-1)^2 + (0.1)^2\right)^{3/2}}. \tag{2.6}$$

All of the results are obtained by transforming f from the standard triangular domain with the nodal offset and applying Gauss-Legendre quadrature in the Q8 space. The integrand of interest is given as:

$$\int_0^1 \int_0^{1-y} f(x,y)\mathrm{d}x\,\mathrm{d}y \tag{2.7}$$

The objective of the nodal-offset technique is to obtain efficiency in terms of the order of quadrature used. In other words, one would like to obtain the same accuracy with fewer quadrature points. Hence convergence and efficiency plots are provided in Figure 2.7.

Perhaps the most interesting observation about the nodal offset technique is that a new sensitivity arises regarding the polynomials associated with the quadrature. Referring to the left plot in Figure 2.7, integrand (2.7) is evaluated with d values spanning from zero to the quarter point and shows multiple local minima. Depending on the goals of the user, it is advised that both of these plots are generated for a given integrand, such that the optimal nodal-offset distance, d, can be chosen. It can be observed that the efficiency gained at higher orders of quadrature is substantial. As an example, when $d = 0.155$ versus $d = 0.15$ for a quadrature order of $n = 30$, roughly four significant figures are gained. The

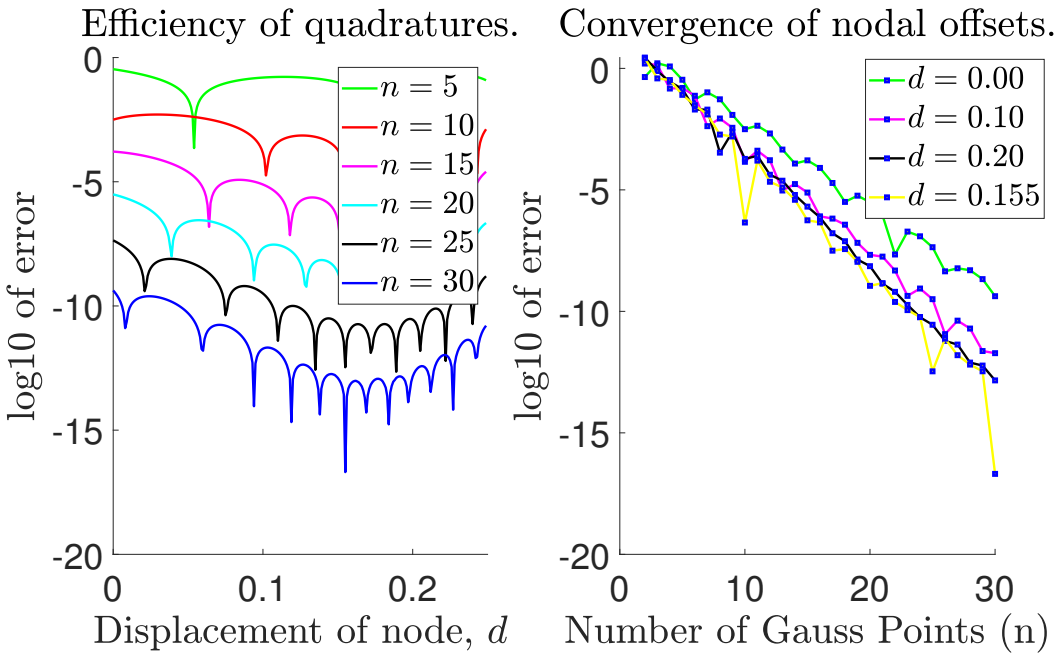

Figure 2.7

Efficiency and convergence of the nodal offset technique are observed for integrand (2.7), for the test case of **corner nodes**. The result for D_{11} shown here (see Figure 2.8).

results suggest that one may seek optimal placement of mid-side nodes, possibly for a given problem.

From the right plot in Figure 2.7, it is observed that, for the optimal nodal-offset distance $d = 0.155$, for the quadrature order $n = 30$, seven significant figures are gained over the standard Duffy transformation ($d = 0$). Additionally, in terms of efficiency, the accuracy of the standard Duffy at $n = 30$ is exceeded at $n = 20$ by using a nodal offset of $d = 0.153$. This means that the number of quadrature points saved is $30^2 - 20^2 = 500$, or 55.5%. However, this is for a specific integrand located on a corner point. To support the value for the general use, the remaining cases of $\mathbf{p}$ across the element are now investigated.

2.4.2 Three Primary Cases of Integration

In practice, one may wish to use interpolating functions of higher order, meaning that $\mathbf{p}$ can appear at locations other than corner nodes. The is addressed by investigating three general locations of placement. The cases of arbitrary locations of a near singularity located on a corner node, an edge node, and an interior node are investigated. The corner node case has already been investigated in Section 2.4.1. The subdivisions are shown in Figure 2.8.

The integral

$$f(x,y) = \frac{1}{\left((x-p_x)^2 + (y-p_y)^2 + (0.1)^2\right)^{3/2}}, \tag{2.8}$$

$$\int_0^1 \int_0^{1-y} f(x,y) \mathrm{d}x \, \mathrm{d}y \tag{2.9}$$

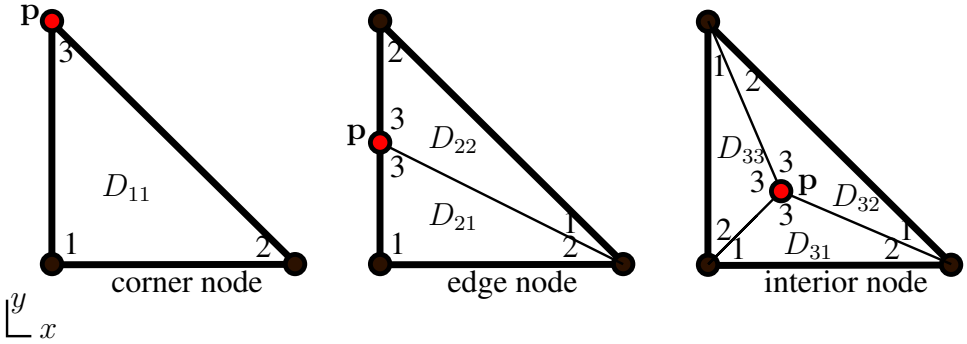

Figure 2.8

Depending on the location of $\mathbf{p}$ relative to the element surface, the domain of the element is to be subdivided. There are three cases for subdivision used here: corner, edge, and interior.

is sought. It should be noted that p_x and p_y are the locations of point $\mathbf{p}$. The locations of each subdomain are given in Table 2.3. Each subdomain is first transformed to the standard triangular domain using the T3 shape functions in EQ. (2.10) [100]. From this standard triangular domain, the nodal offset method is applied for each case.

$$\begin{aligned} N_1 &= 1 - \xi - \eta \\ N_2 &= \xi \\ N_3 &= \eta \end{aligned} \tag{2.10}$$

2.4.2.1 Source Point on Edge

The test case of $\mathbf{p}$ placed on an edge node is investigated. The case of the edge node can be visualized by referencing the "edge node" triangle, in Figure 2.8. The integral

Table 2.3

Nodal locations for the six standard triangular subdomains illustrated in Figures 2.8 and 2.10.

	Node #	x	y		Node #	x	y
D_{11}	Node 1	0	0	D_{41}	Node 1	0.2	0
	Node 2	1	0		Node 2	1	0
	Node 3	0	1		Node 3	0.2	0.3
D_{21}	Node 1	0	0	D_{42}	Node 1	1	0
	Node 2	1	0		Node 2	0.45	0.55
	Node 3	0	0.4		Node 3	0.2	0.3
D_{22}	Node 1	1	0	D_{43}	Node 1	0.45	0.55
	Node 2	0	1		Node 2	0	1
	Node 3	0	0.4		Node 3	0.2	0.3
D_{31}	Node 1	0	0	D_{44}	Node 1	0	1
	Node 2	1	0		Node 2	0	0.3
	Node 3	0.2	0.3		Node 3	0.2	0.3
D_{32}	Node 1	1	0	D_{45}	Node 1	0	0.3
	Node 2	0	1		Node 2	0	0
	Node 3	0.2	0.3		Node 3	0.2	0.3
D_{33}	Node 1	0	1	D_{46}	Node 1	0	0
	Node 2	0	0		Node 2	0.2	0
	Node 3	0.2	0.3		Node 3	0.2	0.3

in EQ. (2.8) with $p_x = 0$, and $p_y = 0.4$ is numerically evaluated using the nodal offset technique. The numerical results for subdomains D_{21} and D_{22} are added together, and the cumulative result is shown. Results are provided in Figure 2.9.

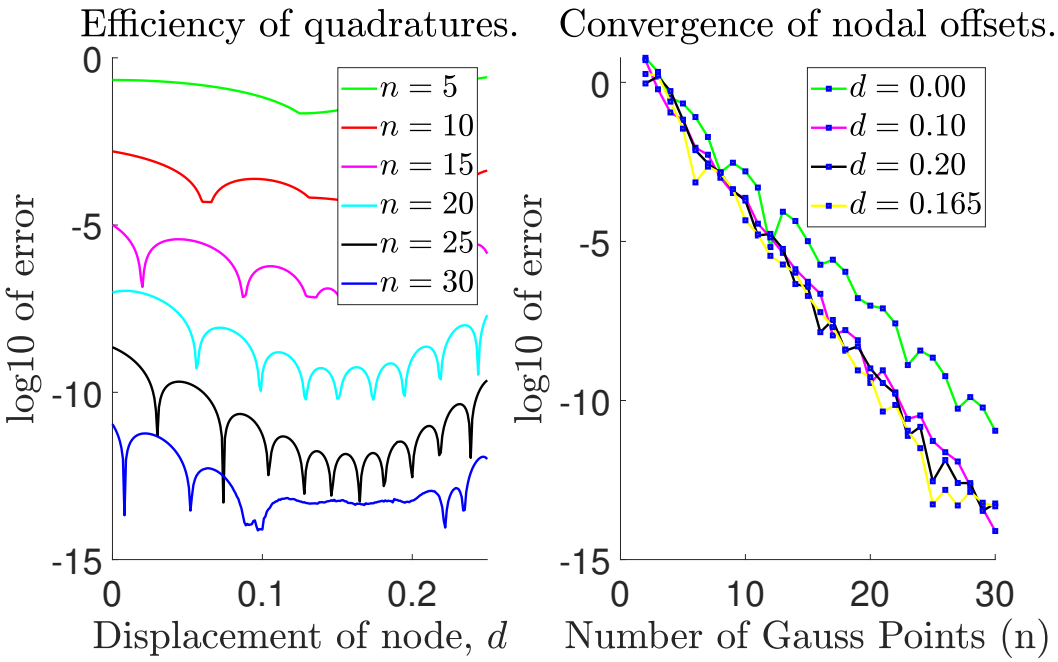

Figure 2.9

Efficiency and convergence of the nodal offset technique are observed for integrand (2.8), where $p_x = 0$ and $p_y = 0.4$, for the test case of **edge nodes**. The cumulative result for D_{21} and D_{22} are shown here.

Figure 2.9 shows similar savings to that of the corner node. The method is shown to work for edge nodes.

2.4.2.2 Source Point on Interior

The test case of $\mathbf{p}$ placed on an interior node is investigated. The case of the interior node can be visualized by referencing the "interior node" triangle, in Figure 2.8. The integral in EQ. (2.8) with $p_x = 0.2$, and $p_y = 0.3$ is numerically evaluated using the nodal offset technique. For the case of an interior $\mathbf{p}$ point, a standard subdivision strategy (as shown in [47]) is often used. However, it has been found that the proposed method requires a further refined subdivision, as shown in Figure 2.10. Under the same conditions of integration, the numerical results for subdomains D_{41} thru D_{46} are added together, and the cumulative result is shown. Results are provided in Figure 2.11.

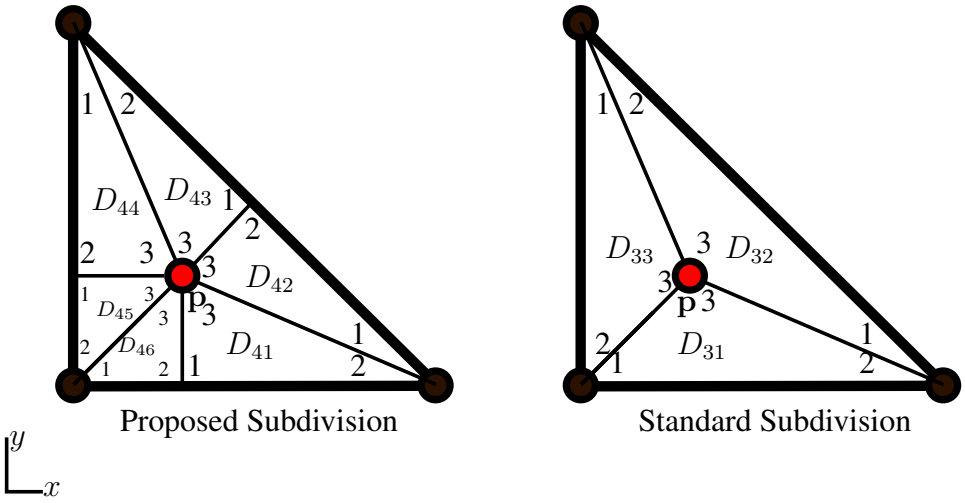

Figure 2.10

It was found that the proposed method requires a more-refined subdivision for interior points. Therefore a refined subdomain is proposed (6 domains).

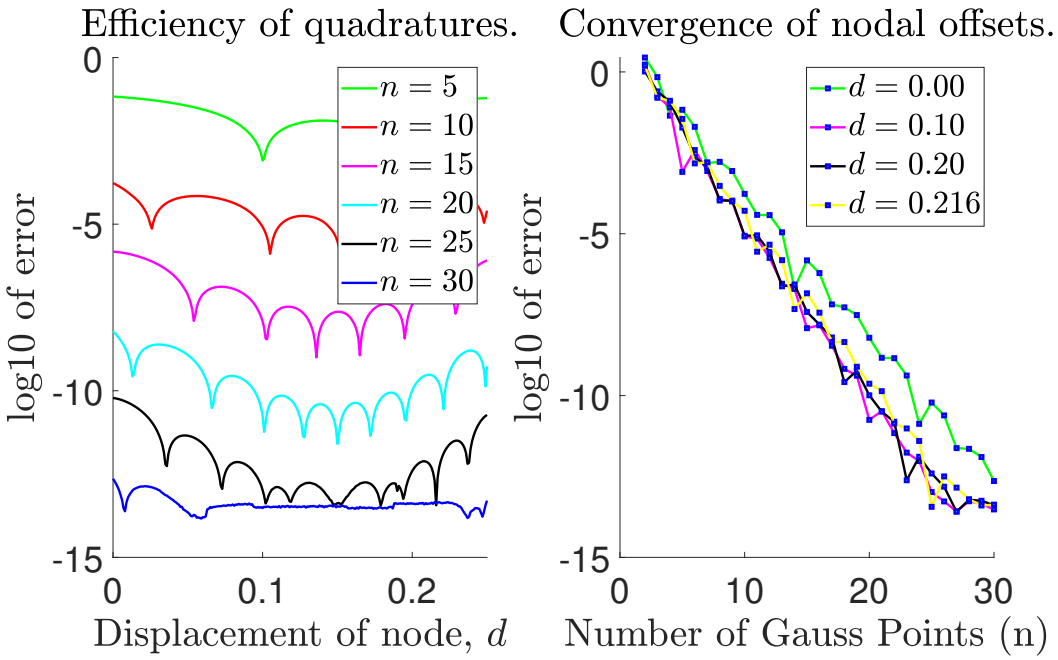

Figure 2.11

Efficiency and convergence of the nodal offset technique are observed for integrand (2.8), for the test case of **interior nodes** with the **proposed subdivision strategy** shown in Figure 2.10. The cumulative result is for D_{41} thru D_{46} are shown here.

Figure 2.11 shows similar savings to that of the corner and edge nodes. The method is shown to work for interior nodes. However, standard subdomaining techniques may need to be refined in order to leverage the method for interior nodes.

2.5 Numerical Example

Thus far, the concept of the nodal-offset technique has been shown to provide strong results for a near hypersingular integrand in a number of general cases. A numerical example of this concept is now applied to the gradient of Green's third identity in the context of the method of functional equations. The integrand for this example is given as,

$$\phi(\mathbf{p})_{,1} = \iint \left(-\psi(\mathbf{p}, \mathbf{Q}_k)_{,1} \frac{\mathrm{d}\,\phi(\mathbf{Q})}{\mathrm{d}\hat{n}} + \phi(\mathbf{Q}) \frac{\mathrm{d}\psi(\mathbf{p}, \mathbf{Q}_k)_{,1}}{\mathrm{d}\hat{n}} \right) \mathrm{dS}(\mathbf{Q}), \tag{2.11}$$

on the surface of $z = 0$, over the standard triangular domain. The source point location, $\mathbf{p}$ is given as [0,1,0.1]. A transcendental, harmonic potential function was chosen based on its ability to serve as a modelling problem, and one that cannot be exactly modeled by polynomials. The function ϕ is given as

$$\phi = e^{0.003z}\sin(0.003x) + e^{0.003x}\sin(0.003y) + e^{0.003y}\sin(0.003z)\,. \tag{2.12}$$

EQ.(2.11) shows the term $\dfrac{\mathrm{d}\psi(\mathbf{p}, \mathbf{Q}_k)_{,1}}{\mathrm{d}\hat{n}}$, which is a near hypersingular kernel of order $1/r^3$. EQ.(2.11) represents a significant modelling challenge when considering the rapidly varying nature of the near strongly singular, near hypersingular kernels, the non-transcendental potential function.

2.5.1 Convergence of Select Offsets

Convergence and efficiency plots for the integrand in EQ. (2.11) are provided in Figure 2.12. Much like the results from the general case, the sensitivity to quadrature order remains, resulting in multiple local minima. The reader is encouraged to interpret both plots simultaneously. Figure 2.12 (left) shows the best nodal offset value, d, for $n = 30$, is associated with $d = 0.209$. For a quadrature order of $n = 30$, the nodal offset technique results in an accuracy improvement of approximately five significant digits, observed on the right in Figure 2.12. Conversely the accuracy of the standard Duffy transformation for $n = 30$ was approximately equaled when $n = 15$ is associated with $d = 0.179$, resulting in a quadrature reduction of $30^2 - 15^2 = 675$ points, or 75%. Thus, the nodal offset technique has been demonstrated to offer significant improvements over a Duffy transformation for an instance of Green's third identity in the context of the direct integration of Kupradze's method of functional equations [50,51]. Additionally, these results appear to compete with many other transformation techniques [47], although different integrands were evaluated. A visualization of the smoothing associated with the nodal offset point $d = 0.209$ is provided in Figure 2.13.

2.6 Conclusion

The present work offers a new transformation technique by offsetting select nodes in a quadratic element shape function transformation. Cases of near hypersingular integrals were investigated, including a practical example of Green's third identity. It was shown that by applying the nodal offset technique to a practical example, quadrature points can

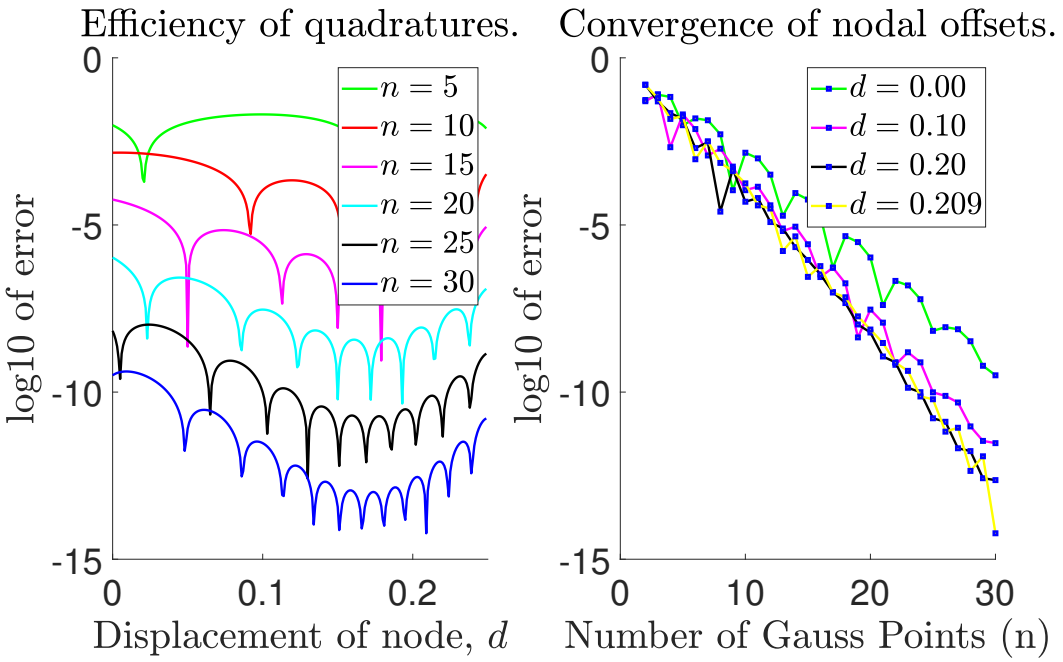

Figure 2.12

Efficiency and convergence of the nodal offset technique are observed for integrand (2.11).

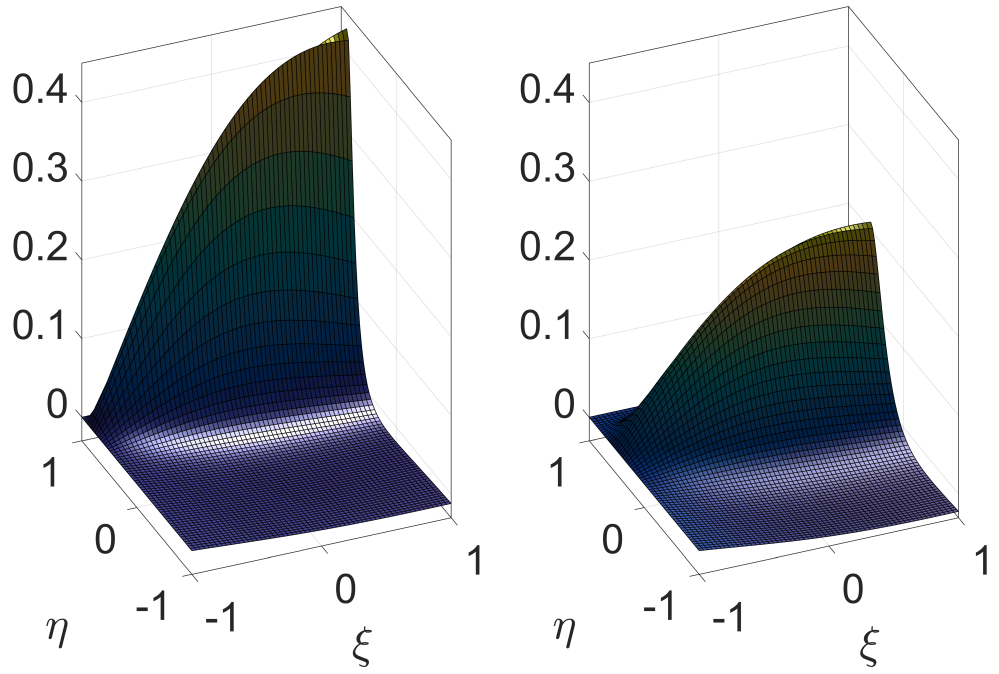

Figure 2.13

A comparison of a zero-nodal offset transformation (left) versus a nodal offset of $d = 0.209$ (right, $n = 30$ minimum point) for EQ. (2.11).

potentially be reduced by 75% while retaining the same accuracy as a standard Duffy technique, or an accuracy improvement of five significant digits over a standard Duffy technique may occur while retaining the same quadrature order. Additionally, the method was shown to be effective in multiple cases of near singularities occurring over an element (corners, edges, interior points).

The method introduces one new degree of freedom, referred to as d, which is used to find an optimum elemental distortion. Numerical investigation of the effect of d showed significant improvements. However, it is suggested that further improvements can be seen by increasing the order of the elements and increasing the degrees of freedom. Should an approach like this be taken, it is likely that a sophisticated optimization could be used to find optimal points in higher dimensions.

Finally, it was observed that the nodal offset technique showed a connection between local minima and quadrature polynomials. A similar study including quadrature obtained from multiple polynomials, and the development of a polynomial under the context of the nodal-offset technique may yield stronger results.

CHAPTER III

EFFICIENT APPROXIMATION OF MULTIVARIATE WEAKLY SINGULAR INTEGRALS BY USING OVER-REGULARIZATION

3.1 Abstract

The present work offers a technique, based on regularization, which allows for a weakly singular integral to be decomposed into two parts: a regular part and a remainder. The regular part is amenable to direct application of a quadrature rule, as the integrand has been smoothed, and effects of the singularity are significantly diminished. The remainder is often in a form which is convenient for closed form integration. This decomposition allows for a hybrid numerical-analytical approach which simplifies the problem of the weakly singular integral, and increases computational efficiency. The method does not require a domain transformation, although it can support one if desired.

3.2 Introduction

Many problems in physics and engineering are governed by partial differential equations (PDEs) [65], which are often addresed with boundary integral methods. The boundary element method (BEM) [7] is one of the most popular methods in this area. Boundary integral methods allow partial differential equations to be cast in the form of integral identities. This results in a gain in computational efficiency by reducing the dimensionality of

the problem. However, this gain in efficiency is offset by increased mathematical complexity. Particularly, boundary integral forms of PDEs will give rise to singular integrals. The boundary form of Green's third identity [23, 46] will contain weakly singular, and strongly singular integrals. The boundary form of the gradient of Green's third identity will also contain hypersingular integrals. Singular integrals occur in most types of BEM problems [1, 27, 29, 62, 63].

There are a number of techniques in the literature for dealing with high order singularities. Most techniques rely on analytical formulæ, which will increase programming complexity as well as limit the order of interpolation used [71]. However, through the use of regularization [4, 13, 71–74, 78, 81, 83, 85, 92, 94], high order singularities can be reduced to weakly singular forms which are suitable for direct numerical integration [19,66,84,86,88]. Therefore, if using regularization, only techniques regarding weakly singular integrals are required for a boundary integral problem.

The present work extends the concept of regularization by proposing a hybrid technique. The technique presented represents the weakly singular integral as a combination of closed form expressions and a smoothed integrand suitable for numerical evaluation. Concepts and examples are provided within.

3.3 Regularization

The present work is concerned with two-dimensional, weakly singular integrals, although the same concept can easily be extended to one-dimensional integrals. This work presents the weakly singular integral in the form

$$\iint_A \frac{f(x,y)}{\sqrt{(x-x_0)^2+(y-y_0)^2}}\,\mathrm{d}x\,\mathrm{d}y = \iint_A \frac{f(x,y)}{r}\,\mathrm{d}A, \tag{3.1}$$

where x_0 and y_0 are on A. In the context of singular integrals, regularization can be viewed as an efficient and effective way to reduce the order of a singularity. An effective way of regularizing an integral is to use Taylor's theorem to represent f in the neighborhood of the singularity at (x_0, y_0), and then subtract this result from the integrand. Subtracting a first-order Taylor series (a constant) is a "one-term regularization." Subtracting a second-order Taylor series (a linear state approximation) is a "two-term regularization," and so on. This results in a decomposition of the integral into a part suitable for closed form integration, and a part suitable for numerical integration. Similar decomposition techniques have been used in other works [22, 28, 44, 57, 89]. As a note, a two-term regularization applied to a hypersingular integral would bring the singularity from $\mathscr{O}\left(1/r^3\right)$ to $\mathscr{O}\left(1/r\right)$, which is a weakly singular integral in a three-dimensional BEM problem. Any regularization beyond the weakly singular form is considered over-regularization.

Over-regularization of a weakly singular integral results in a smoother integrand. The resulting integral is much more amenable to a direct quadrature rule than a weakly singular integral. Additionally, over-regularization requires no domain or variable transformations.

3.3.1 Demonstration of Smoothing Effects

As a demonstration of concept, one can consider the regularization of the weakly singular integral

$$I = \iint_A \frac{e^{xy}}{\sqrt{(x-x_0)^2 + (y-y_0)^2}} \, \mathrm{d}x \, \mathrm{d}y = \iint_A \frac{e^{xy}}{r} \, \mathrm{d}A. \tag{3.2}$$

Subtracting a Taylor series approximation from integral 3.2 reduces the effect of the singularity. The subtracted remainder must then be added back. As the order of regularization increases, the regularized part becomes smoother and smaller in magnitude in comparison to the remainder. In other words, the remainder will typically represent the larger percentage of the integrand as more steps of over-regularization are performed. As a visual representation of the regularizing effect, the regularized parts of EQ. (3.8) are provided in Figures 3.1 and 3.2.

3.3.2 Handling the Remainder Terms

Figures 3.1 and 3.2 demonstrate that regularization can be used for a smoothing effect. This indicates that the regularized part of the integral is suitable for direct application of quadrature. However the issue of handling the remainder terms remains (see the remainder terms in EQ. (3.8)). One does have the option to numerically integrate the remainder, but modern symbolic packages can compute these integrals in closed form (e.g. Maple).

The regularization process provided here uses a Taylor series expansion at the singularity located at (x_0, y_0) which will always appear in a form resembling,

$$f(x,y) \approx \text{Taylor}\left(f(x_0,y_0)\right) = c_1 + c_2 x + c_3 y + c_4 xy + c_5 x^2 + c_6 y^2 + \ldots. \tag{3.3}$$

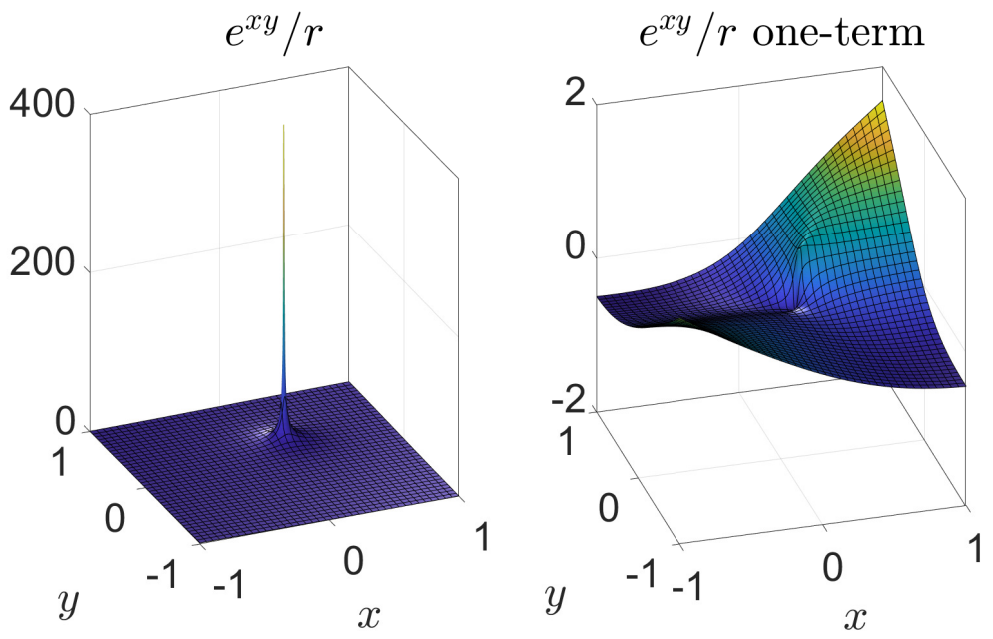

Figure 3.1

A one-term regularization (right) is applied to integral 3.2, $(x_0,\ y_0) = (0.2, 0.3)$. Note that the resulting integrand for the one-term regularization no longer approaches infinity at the singularity. The one-term plot only shows the regularized part of the integral.

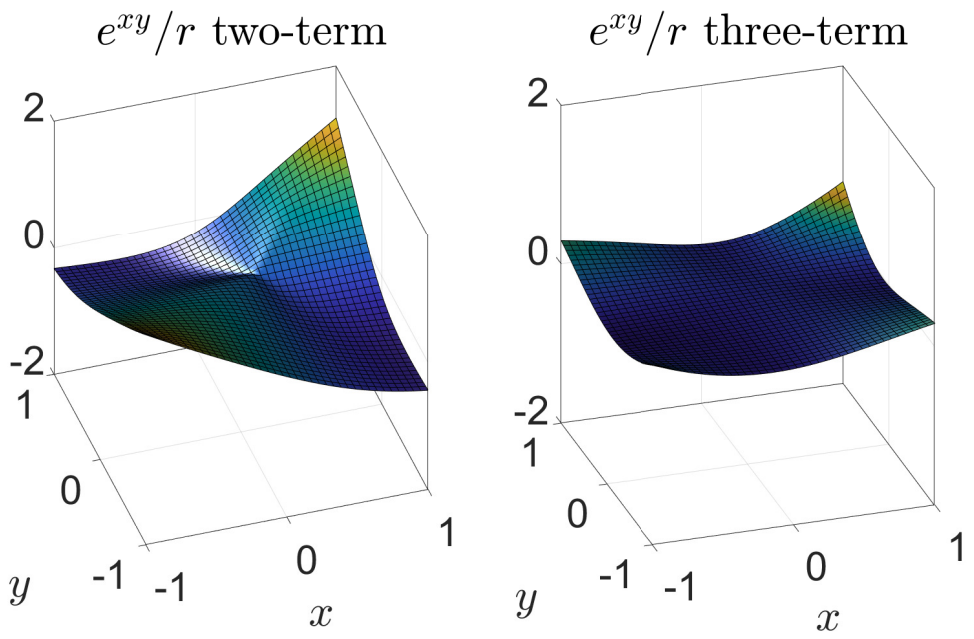

Figure 3.2

A two-term regularization (left) and a three-term regularization (right) are applied to integral 3.2, $(x_0,\ y_0) = (0.2, 0.3)$, and are provided here. Note that the effect of the singularity continues to diminish as higher steps of over-regularization are taken. The two and three-term plots only show the regularized parts of the integral.

This indicates that the remainder can be represented as

$$\begin{aligned}\text{Remainder} = c_1 \iint_A \frac{1}{r}\,\mathrm{d}A + c_2 \iint_A \frac{x}{r}\,\mathrm{d}A + c_3 \iint_A \frac{y}{r}\,\mathrm{d}A \\ + c_4 \iint_A \frac{xy}{r}\,\mathrm{d}A + c_5 \iint_A \frac{x^2}{r}\,\mathrm{d}A + c_6 \iint_A \frac{y^2}{r}\,\mathrm{d}A + \ldots\end{aligned} \tag{3.4}$$

The full form of a two-term regularization can therefore be presented as

$$\underbrace{\iint_A \frac{f(x,y) - c_1 - c_2 x - c_3 y}{r}\,\mathrm{d}A}_{\text{Regularized part}} + \underbrace{c_1 \iint_A \frac{1}{r}\,\mathrm{d}A + c_2 \iint_A \frac{x}{r}\,\mathrm{d}A + c_3 \iint_A \frac{y}{r}\,\mathrm{d}A.}_{\text{Remainder}} \tag{3.5}$$

The form of the remainder offers a certain convenience. It should be observed the remainder will always appear in the form of a vector of constants dotted into a vector of specific integrals. The constants follow from the Taylor series expansion, while the integrals can be evaluated in closed form. This dot-product form is convenient for programming.

The downside of closed-form solutions is that they will significantly lengthen the run time of a computer code. However, this issue can be circumvented by storing the values of these integrals at nodes across an element. Once the closed form values are stored, they can be called from a data file. Conversely, one can store numerical solutions to these integrals.

3.4 Order of Regularization Required

Choosing how many steps of over-regularization are desired for an integral is a choice depending on several factors. Considerations regarding these factors are provided.

As mentioned previously, as the order of over-regularization increases, so does the remainder of the integral. In other words, the remainder approaches the true solution to the original integral with high orders of over-regularization. Another way of thinking of this, is that significant increases in accuracy are gained with each step of over-regularization.

If one so chooses, a Taylor series can be expanded so far that the regularized part of the integral is negligible in comparison to that of the remainder. Therefore, the user could conceivably eliminate quadrature all together, and store a database of closed-form integrals instead. However, it is assumed that a hybrid approach will typically be taken by the user.

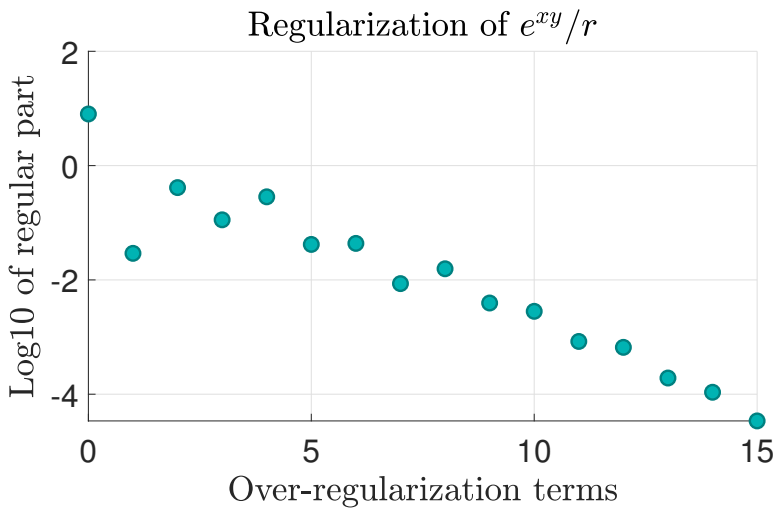

Figure 3.3

The effect of the regularized part of the integral trending downward in size is shown. Note that as the more Taylor terms are subtracted from the integral, the regularized part becomes smaller.

Figure 3.3 demonstrates the effect of convergence due to over-regularization. It can be seen that as more regularization terms are subtracted from the integrand, the regularized portion of the integral will trend downward in size. This indicates that at some point, the remainder portion of the integral will represent most of the integral, and the regularized portion will be negligible. The rate of this convergence also depends on how well the

Taylor series expansion can model $f(x, y)$ with a given number of terms. A function that is more-easily approximated (i.e. well approximated with fewer terms) will have a faster convergence than a highly non-linear function.

Perhaps the important point to take from this discussion is that the accuracy of the method will depend on two key factors. The first factor is that each step of over-regularization will result in additional smoothing for the regularized portion of the integral. This means that with each step, the ability for quadrature to capture the effects of the integrand will improve. The second factor is the fact that significant figures are also gained by the remainder trending to a larger portion of the integral as the order of over-regularization becomes higher. How much each of these factors contributes to accuracy will depend on the nature of the integrand (i.e. how well it is captured by a Taylor series of few terms).

3.5 Numerical Examples

3.5.1 Straight-Sided Element Example

The first numerical example is performed on a square, flat, straight-sided element. Elements of this type will yield constant Jacobians of the transformation, as well as linear expressions for the transformed coordinates. This will result in the general form of the integral remaining in-tact through the domain transformation process.

For this example, the weakly singular integral

$$\int_{-1}^{1}\int_{-1}^{1} \frac{e^{xy}}{\sqrt{(x-0.2)^2+(y-0.3)^2}} \mathrm{d}x\,\mathrm{d}y \approx 7.260661531 \tag{3.6}$$

is evaluated over the standard Q4 element space. The approximate value of this integrand was found by using a Duffy transformation [19] with four subdomains over the Q4

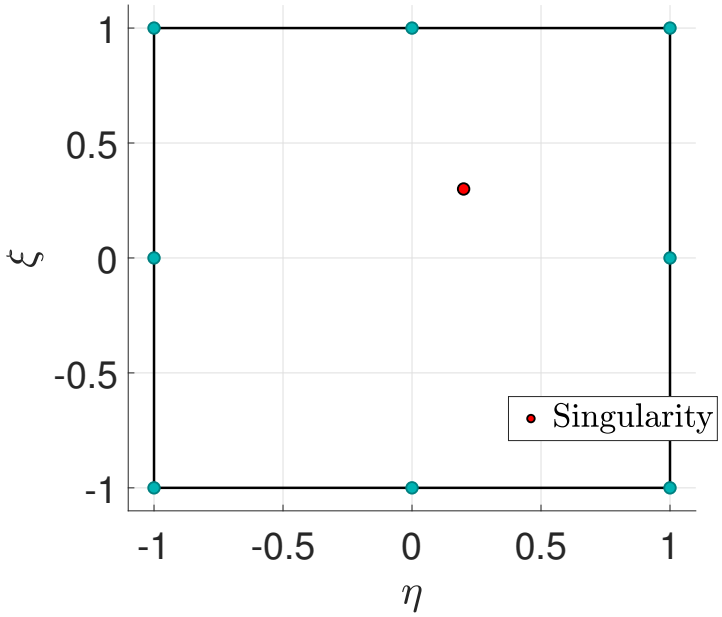

Figure 3.4

The domain for the straight-sided element example is provided here. This domain is a unit square, which is a standard Q4 element domain. Note the singularity placed at (0.2, 0.3). This domain is associated with integral 3.6.

space. Each subdomain was evaluated with a 512x512 point Gauss-Legendre quadrature rule. Only ten significant figures were used here, to ensure accuracy of the approximated numbers.

In order to regularize integral 3.6, Taylor series expansions must be found for each case. As an example, the one, two, and three-term Taylor series expansions for e^{xy} at $(0.2, 0.3)$ are

$$\begin{aligned}
\text{One Term} &= e^{3/50}, \\
\text{Two Term} &= \frac{22e^{3/50}}{25} + \frac{3e^{3/50}}{10}x + \frac{e^{3/50}}{5}y, \\
\text{Three Term} &= \frac{592e^{3/50}}{625} - \frac{9e^{3/50}}{250}x - \frac{3e^{3/50}}{125}y + \frac{53e^{3/50}}{50}xy + \frac{9e^{3/50}}{200}x^2 + \frac{e^{3/50}}{50}y^2.
\end{aligned} \tag{3.7}$$

The one, two, and three-term regularizations of integral 3.6, respectively, are,

$$\begin{aligned}
I &= \iint_A \frac{e^{xy} - e^{3/50}}{r}\,\mathrm{d}A + \iint_A \frac{e^{3/50}}{r}\,\mathrm{d}A \\
I &= \iint_A \frac{e^{xy} - \frac{22e^{3/50}}{25} - \frac{3e^{3/50}}{10}x - \frac{e^{3/50}}{5}y}{r}\,\mathrm{d}A + \iint_A \frac{\frac{22e^{3/50}}{25} + \frac{3e^{3/50}}{10}x + \frac{e^{3/50}}{5}y}{r}\,\mathrm{d}A \\
I &= \underbrace{\iint_A \frac{e^{xy} - \frac{592e^{3/50}}{625} + \frac{9e^{3/50}}{250}x + \frac{3e^{3/50}}{125}y - \frac{53e^{3/50}}{50}xy - \frac{9e^{3/50}}{200}x^2 - \frac{e^{3/50}}{50}y^2}{r}\,\mathrm{d}A}_{\text{Regularized part}} \\
&\quad + \underbrace{\iint_A \frac{\frac{592e^{3/50}}{625} - \frac{9e^{3/50}}{250}x - \frac{3e^{3/50}}{125}y + \frac{53e^{3/50}}{50}xy + \frac{9e^{3/50}}{200}x^2 + \frac{e^{3/50}}{50}y^2}{r}\,\mathrm{d}A.}_{\text{Remainder}}
\end{aligned} \tag{3.8}$$

Over-regularization was performed with terms varying from zero to ten. For the numerical example, quadrature was held at a 10x10 (100 point) rule, as over-regularization was increased. A 100 point Duffy rule [19] was used for step 0 as a benchmark. Errors and significant digits are reported in Table 3.1.

Table 3.1

Numerical results for the over-regularization of integral 3.6 are provided. Accuracy increases as more over-regularization terms are taken.

Straight-Sided Element Case (100 point quadrature rule)		
Regularization Order	Absolute Percent Error	Significant Digits
(Duffy Method) 0	$1.27(10^{-2})$	2
1	$4.66(10^{-2})$	2
2	$2.9(10^{-3})$	4
3	$6.42(10^{-4})$	5
4	$5.72(10^{-5})$	6
5	$2.26(10^{-5})$	6
6	$9.14(10^{-7})$	8
7	$3.73(10^{-7})$	8
8	$1.05(10^{-8})$	9
9	$2.65(10^{-8})$	8
10	$2.11(10^{-9})$	10

Table 3.1 demonstrates that the regularization method can significantly outperform a standard Duffy method [19] as more terms are taken. Accuracy is limited only by how many over-regularization terms one wishes to use.

3.5.2 Curved Element Example

The second numerical example is performed on a quadratic-approximated circle, curved Q8 element. Nodal locations are taken at 45 degree intervals along the unit circle. The domain is bounded by quadratic polynomials arising from the Q8 shape functions. This element is transformed from the physical domain (x, y) to the standard Q4 space (ξ, η) for numerical integration. Figure 3.5 is provided for a visualization of the domain.

For simplicity, the singularity was placed at the origin at $(x_0, y_0) = (0, 0)$. The weakly singular integral for this example is

$$\begin{aligned} &\iint_A \frac{e^{xy}}{\sqrt{x^2+y^2}} \mathrm{d}x\, \mathrm{d}y \approx 6.322255060 \\ &= \int_{-1}^{1}\int_{-1}^{1} \frac{\exp\left[\left(\eta - \eta\xi^2 + \frac{1}{2}(\sqrt{2}\eta\xi^2)\right)\left(-\xi + \eta^2\xi - \frac{1}{2}(\sqrt{2}\eta^2\xi)\right)\right]}{\sqrt{\left(\eta - \eta\xi^2 + \frac{1}{2}(\sqrt{2}\eta\xi^2)\right)^2 + \left(-\xi + \eta^2\xi - \frac{1}{2}(\sqrt{2}\eta^2\xi)\right)^2}} J(\xi,\eta)\, \mathrm{d}\xi\, \mathrm{d}\eta, \end{aligned} \tag{3.9}$$

where the Jacobian of the transformation is,

$$J(\xi,\eta) = \left(\frac{1}{2}\left(\sqrt{2}\eta^2\right) - \eta^2 + 1\right)\left(\frac{1}{2}\left(\sqrt{2}\xi^2\right) - \xi^2 + 1\right) - \left(2\eta\xi - \sqrt{2}\eta\xi\right)^2. \tag{3.10}$$

For convenience, the transformed r is now denoted as r_t,

$$r_t = \sqrt{\left(\eta - \eta\xi^2 + \frac{1}{2}(\sqrt{2}\eta\xi^2)\right)^2 + \left(-\xi + \eta^2\xi - \frac{1}{2}(\sqrt{2}\eta^2\xi)\right)^2}, \tag{3.11}$$

and the transformed function $f = e^{xy}$ is now denoted as f_t,

$$f_t = J(\xi,\eta)\, \exp\left[\left(\eta - \eta\xi^2 + \frac{1}{2}(\sqrt{2}\eta\xi^2)\right)\left(-\xi + \eta^2\xi - \frac{1}{2}(\sqrt{2}\eta^2\xi)\right)\right]. \tag{3.12}$$

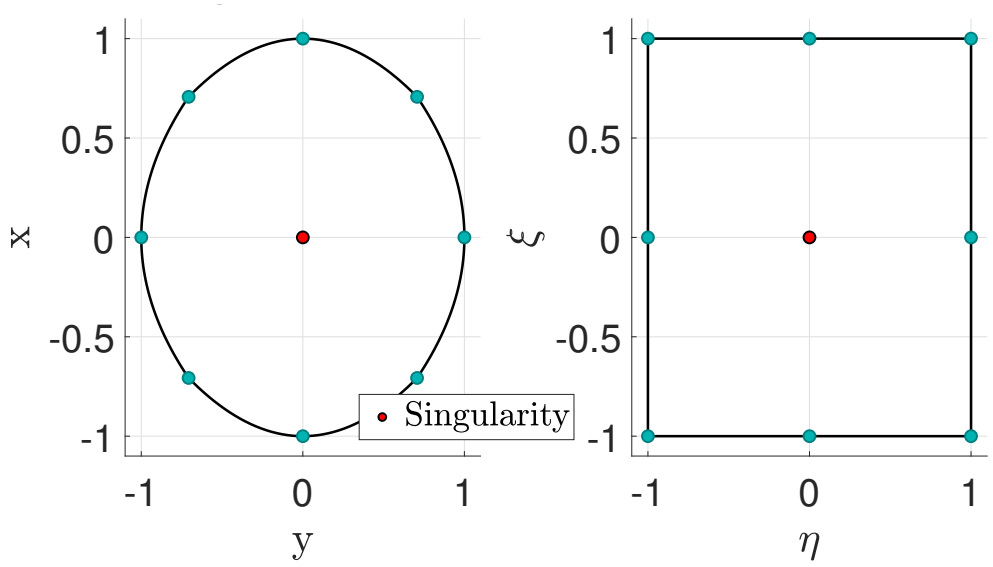

Figure 3.5

A curved Q8 element was used in the transformation of integral 3.9 into a standard Q4 domain. Note that the original domain (left) is bounded by quadratic polynomials which approximate the unit circle. The curves depicted are only approximations falling from a Q8 element.

The regularized form of integral 3.9 is therefore,

$$\underbrace{\int_{-1}^{1}\int_{-1}^{1}\frac{f_t-\text{Taylor}\left(f_t\left(x_0,y_0\right)\right)}{r_t}\mathrm{d}\xi\,\mathrm{d}\eta}_{\text{Regularized Part}}+\underbrace{\int_{-1}^{1}\int_{-1}^{1}\frac{\text{Taylor}\left(f_t\left(x_0,y_0\right)\right)}{r_t}\mathrm{d}\xi\,\mathrm{d}\eta}_{\text{Remainder}} \tag{3.13}$$

The approximate value of integral 3.9 was found by using a Duffy transformation [19] with four subdomains over the Q4 space. Each subdomain was evaluated with a 512x512 point Gauss-Legendre quadrature rule. Only ten significant figures were used here, to ensure accuracy of the approximated numbers.

Integral 3.9 shows that r is no longer in a convenient form, and that a complicated Jacobian is now attached to $f(\xi,\eta)$. However, this has no bearing on the regularization process, as long as the same denominator is used for regularization. In other words, the process of regularization can be applied directly in the same way as the straight sided element case, except the transformed r, r_t, must be used as the denominator. The downside to using this method for curved elements is that remainder terms are unlikely to be found in closed form. However, they will still remain in the form depicted in EQ. 3.4. Therefore, the concept of storing these integrals can still be preserved, but they must be evaluated numerically, or in closed form in the original domain.

Multi-term regularization has been applied to the integrand in 3.9 and shown in Figures 3.6 and 3.7.

Numerical results for integral 3.9 are provided in Table 3.2. Note that only odd numbers of regularization were used, as Taylor series terms were zero for the even-numbered trials. This follows from the fact that r was centered at (0,0).

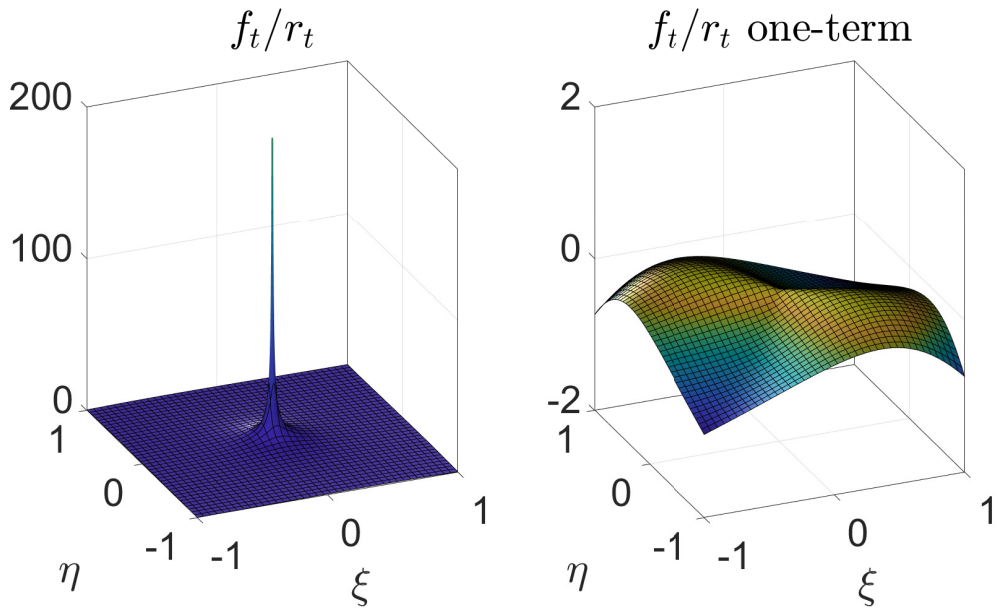

Figure 3.6

A one-term regularization (right) is applied to integral 3.9 in the transformed space. The domain pictured is associated with the "transformed domain" in Figure 3.5. The remainder is not visualized here.

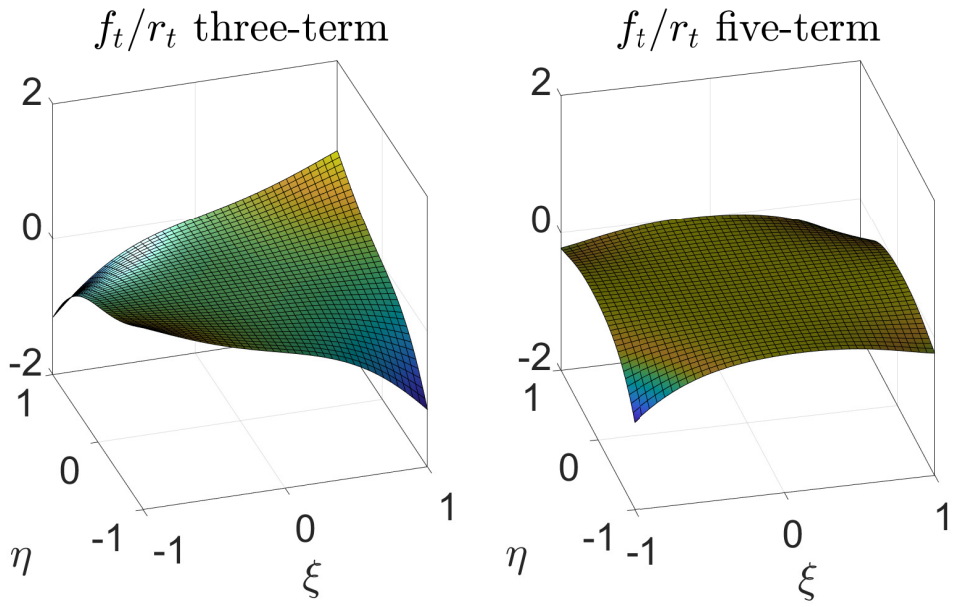

Figure 3.7

A three-term regularization (left), and a five-term regularization (right) are applied to integral 3.9 in the transformed space. The domain pictured is associated with the "transformed domain" in Figure 3.5. The remainders are not visualized here.

Table 3.2

Numerical results for the over-regularization of integral 3.9 are provided. Accuracy increases as more over-regularization terms are taken.

Curved Element Case (100 point quadrature rule)		
Regularization Order	Absolute Percent Error	Significant Digits
(Duffy Method) 0	$2.74(10^{-3})$	3
1	$8.45(10^{-3})$	2
3	$3.34(10^{-4})$	4
5	$1.29(10^{-5})$	7
7	$2.85(10^{-7})$	8
9	$9.01(10^{-9})$	8

It is shown from these results that the method works well for both straight-sided and curved elements, and is suitable as a general purpose integration method. Additionally, no accuracy appeared to be lost for the curved case.

3.6 Conclusion

The present method offers a new technique, based on regularization, which allows for a weakly singular integral to be decomposed into two parts, one of the parts to be integrated numerically, and the other in closed form. The method uses over-regularization and offers a combination of integral smoothing and reduction in integral magnitude.

Practical examples on a straight-sided element and a curved element showed that the method is effective, accurate, and suitable for general purpose use. Additionally, the

method was able to outperform the Duffy transformation [19] for both cases. The method also shows versatility in that one may conceivably use high order regularizations as a replacement of quadrature rules.

CHAPTER IV

THE USE OF HIGH ORDER ELEMENTS IN THE BOUNDARY ELEMENT METHOD WITH REGULARIZATION

4.1 Abstract

The present work investigates a modification of the boundary element method which uses regularization to reduce a hypersingular form to a weakly singular form. This technique allows for boundary integral equations to receive a direct application of numerical quadrature, completely removing the need for closed form integration techniques. This technique also allows the boundary element method to support high order interpolations, allowing for substantial gains in computational efficiency.

4.2 Introduction

The boundary element method (BEM) is an efficient numerical method which is now approaching sixty years of development. Its roots are in potential theory, [38, 38, 46, 91], but it was further popularized by Rizzo [77] and Cruse [11, 12, 14, 15, 17, 90] for their work in elastostatics, elastodynamics, and fracture. From the beginning of its development, the treatment of singular integrals has remained a focal point for the BEM's progress and accessibility. This work will demonstrate that singular integrals can be treated in a favorable, efficient, and simple way by using regularization [78]. More notably, this work

will demonstrate that regularization will remove existing limitations for the BEM and pave the way for substantial computational efficiency by providing the BEM support for high order interpolations.

4.2.1 The Case for a p-version BEM

The overwhelming majority of works that have been published in the area of boundary integral methods, specifically regarding techniques that directly integrate across the surface, use a formulation based on constant, linear, or quadratic, isoparametric elements (for examples see, [33, 68, 69, 80], although there are many more). These formulations often depend on the use of closed-form integration to evaluate singular integrals arising in the boundary integral equations.

Researchers in the area of boundary integral methods who rely on closed-form integration formulæ have limited themselves to the use of low order elements. This is largely due to the difficulty associated with integrating hypersingular kernels in integrals with variation in the spatial domain and in the density higher than quadratic. In three dimensions, the difficulty of this task increases. As a result, the highest order element that has been used in three dimensions is almost always quadratic [31, 52, 94]. One exception is the conference paper by Richardson and Arjunon in 2009 [72], which uses a similar technique to the one used in this work.

By relying on analytical integration, researchers are limited to low-order polynomials to model what may be a rapidly varying density. This results in an inefficient algorithm from a computational standpoint, given the dense nature of BEM systems. In other words,

by only using quadratic elements, a significant increase in system size is required to capture the behavior of the surface density. If a rapidly varying surface density exists over a large surface (e.g. a boat hull), the use of low order polynomials may result in system sizes which approach the limits of modern computational power.

To address this issue, this work suggests using a p-version of the BEM. There have been some instances of p-version research in the BEM [3, 18, 32, 59, 71–73]. With the exception of Richardson and Arjunon [72], it appears that the entirety of these studies have been limited to two dimensions, and three-dimensional applications within the BEM literature are not found. In [72], Richardson and Arjunon successfully used a three-dimensional locally regularized p-version of the BEM. In [71], Richardson applied the simple solutions technique in two-dimensions and demonstrated h-p convergence for high order elements in the BEM. Richardson showed that by employing a p-version BEM, errors can be reduced by several orders of magnitude while also reducing system size. This work seeks to extend this advantage to three-dimensions.

4.3 Modifying the BEM to Support High Order Elements with Regularization

Laplace's equation is,

$$\nabla^2 \phi = 0. \tag{4.1}$$

The Green's function, also known as the fundamental solution, for Laplace's equation in three dimensions is,

$$\psi(\mathbf{P}, \mathbf{Q}) = \frac{1}{4\pi r(\mathbf{P}, \mathbf{Q})}. \tag{4.2}$$

Green's third identity, for Laplace's equation, written on the boundary of a three-dimensional geometry, can therefore be stated in the form

$$\frac{1}{2}\phi(\mathbf{P}) = \iint_{\mathrm{S}} \left(\psi(\mathbf{P},\mathbf{Q}) \frac{\mathrm{d}\,\phi(\mathbf{Q})}{\mathrm{d}\hat{n}(\mathbf{Q})} \right) \mathrm{dS}(\mathbf{Q}) - \overset{\mathrm{CPV}}{\iint_{\mathrm{S}}} \left(\phi(\mathbf{Q}) \frac{\mathrm{d}\psi(\mathbf{P},\mathbf{Q})}{\mathrm{d}\hat{n}(\mathbf{Q})} \right) \mathrm{dS}(\mathbf{Q}). \quad (4.3)$$

and its gradient is often dotted with the normal at $\mathbf{P}$,

$$\frac{1}{2}\frac{\mathrm{d}\phi(\mathbf{P})}{\mathrm{d}\hat{n}(\mathbf{P})} = \overset{\mathrm{CPV}}{\iint_{\mathrm{S}}} \left(-\frac{\mathrm{d}\psi(\mathbf{P},\mathbf{Q})}{\mathrm{d}\hat{n}(\mathbf{P})} \frac{\mathrm{d}\phi(\mathbf{Q})}{\mathrm{d}\hat{n}(\mathbf{Q})} \right) \mathrm{dS}(\mathbf{Q}) + \overset{\mathrm{HFP}}{\iint_{\mathrm{S}}} \left(\phi(\mathbf{Q}) \frac{\mathrm{d}^2\psi(\mathbf{P},\mathbf{Q})}{\mathrm{d}\hat{n}(\mathbf{P})\mathrm{d}\hat{n}(\mathbf{Q})} \right) \mathrm{dS}(\mathbf{Q}). \quad (4.4)$$

where

- $\phi(\mathbf{P})$ represents a potential function in three-dimensions,
- $\phi(\mathbf{Q})$ represents the surface density,
- $\psi(\mathbf{P},\mathbf{Q})$ is the Green's function in three dimensions (also known as the fundamental solution),
- $\mathbf{P}$ and $\mathbf{Q}$ are the source and field points, respectively.

Knowing that ψ is $1/4\pi r$, it is seen that EQ. (4.3) contains weakly singular $\mathscr{O}\left(1/r\right)$, and strongly singular $\mathscr{O}\left(1/r^2\right)$ kernels. Additionally, EQ. (4.4) contains strongly singular $\mathscr{O}\left(1/r^2\right)$, and hypersingular $\mathscr{O}\left(1/r^3\right)$ kernels. As presented, the singular integrals do not exist in the ordinary sense, and must be interpreted as Cauchy principal value (strongly singular case), and Hadamard finite part integrals (hypersingular case), respectively. Without modification, direct application of Gaussian quadrature will fail. The exception is for the weakly singular integral, which is finite and can be evaluated with special quadrature rules [19, 66, 84, 86, 88]. the procedure of integrating these in closed form limits the degree of interpolation that can be applied to ϕ, as it remains a research problem on how to do this for higher degrees of interpolation.

Regularization may be thought of as a class of techniques which effectively reduce the singularity in an integral. The technique employed in this work is the simple solutions method, originally proposed by Rudolphi [78]. The simple solutions method states that singular integrals can be regularized by subtracting a Taylor series approximation of the density at the point of the singularity. The simple solutions method can also be thought of as taking the difference of two boundary integral equations for two different boundary value problems. One problem is the problem of interest, and the other is a linear state problem with matching flux and potential at **P**. This method is an extension of the free-term regularization shown by Cruse [16]. Both forms will be shown here.

4.3.1 One-Term Regularization of Green's Third Identity

Consider a boundary value problem governed by Laplace's equation, such as EQ. (4.3). Knowing that $\psi = {}^{1}/_{4\pi r}$, it can be seen that the derivative of this term results in a strongly singular integral.

Consider a separate boundary value problem, also governed by Laplace's equation, where the potential (ϕ) for this separate problem, is a constant represented by,

$$\phi^C(\mathbf{Q}) = \phi(\mathbf{P}). \tag{4.5}$$

Its gradient is

$$\vec{\nabla}\phi^C(\mathbf{Q}) = 0. \tag{4.6}$$

This term is similar to the rigid body term discussed in [76]. By taking the difference of these two problems, the regularized density will equal zero at **P**, and the singularity will be

reduced by one. Hence, the resulting regularized (weakly singular) form of Green's third identity is,

$$0 = \iint_{\mathrm{S}} \left(\psi(\mathbf{P},\mathbf{Q}) \frac{\mathrm{d}\phi(\mathbf{Q})}{\mathrm{d}\hat{n}(\mathbf{Q})} - \left(\phi(\mathbf{Q}) - \phi^{C}(\mathbf{Q})\right) \frac{\mathrm{d}\psi(\mathbf{Q})}{\mathrm{d}\hat{n}(\mathbf{Q})} \right) \mathrm{dS}(\mathbf{Q}), \tag{4.7}$$

where $\mathrm{d}\psi(\mathbf{Q})/\mathrm{d}\hat{n}(\mathbf{Q})$ is a function of $1/r^2$.

4.3.2 Two-Term Regularization of Green's Third Identity

In a similar fashion to the one term regularization, one can regularize the gradient of Green's third identity by subtracting a separate boundary value problem. This problem is also governed by Laplace's equation and has the linear potential,

$$\phi^{L}(\mathbf{Q}) = \phi(\mathbf{P}) + \vec{\nabla}\phi(\mathbf{P}) \cdot \vec{r}(\mathbf{P},\mathbf{Q}), \tag{4.8}$$

$$\vec{\nabla}\phi^{L}(\mathbf{Q}) = \vec{\nabla}\phi(\mathbf{P}). \tag{4.9}$$

By subtracting this density, the slope is also regularized at point $\mathbf{P}$, resulting in the hyper singularity being reduced by two orders, to a weak singularity. Additionally, the strongly singular integral is regularized by the gradient, which essentially acts as a one-term regularization, resulting in a singularity reduction of one order, to a weak singularity. The regularized, weakly singular form is given as,

$$0 = \iint_{\mathrm{S}} \left(-\frac{\mathrm{d}\psi(\mathbf{P},\mathbf{Q})}{\mathrm{d}\hat{n}(\mathbf{P})} \frac{\mathrm{d}\left(\phi(\mathbf{Q}) - \phi^{L}(\mathbf{Q})\right)}{\mathrm{d}\hat{n}(\mathbf{Q})} + \left(\phi(\mathbf{Q}) - \phi^{L}(\mathbf{Q})\right) \frac{\mathrm{d}^2\psi(\mathbf{P},\mathbf{Q})}{\mathrm{d}\hat{n}(\mathbf{P})\mathrm{d}\hat{n}(\mathbf{Q})} \right) \mathrm{dS}(\mathbf{Q}). \tag{4.10}$$

It should also be noted that applying the two-term regularization to EQ. (4.7) results in over-regularization, which will further reduce the effects of the singularity and leave a smoother integrand.

4.3.3 Support of High Order Interpolations

The regularized forms for Green's third identity and its gradient are presented in their weakly singular forms in EQs. (4.10) and (4.7). It should be noted that the strong and hyper singularities have now been removed from the integrands. This allows these integrals to be evaluated with direct quadrature rules, completely removing the need for any closed form integration techniques. Furthermore, since closed form integration is no-longer needed to evaluate these integrals, the obstacle preventing higher interpolations is now removed. Hence, the regularized forms now offer direct application of quadrature, and direct support of high order elements.

A number of works have employed the simple solutions technique [4, 13, 31, 53–55, 73, 79, 82, 96], but few have exploited the fact that it allows for direct support of high order elements. While there are select examples of researchers performing direct computation of singular integrals by leveraging regularization techniques, even the most sophisticated three-dimensional formulations are typically computing regularized integrals on low-order elements.

The primary motivation of this work is to show the value in the use of high order elements within the context of three-dimensional boundary integral methods. One may question why the p-version is not used for the BEM if it has received successful (albeit limited) treatment in the past.

4.3.4 Controversy Surrounding the Simple Solutions Method

Arguably, one primary reason that a regularized, p-version formulation of the BEM has not taken hold as a popular option is due to criticisms of the simple solutions method [60, 61, 70]. In 1992, Krishnasamy published the first in a series of articles focusing on continuity requirements in hypersingular integral equations [49]. This sparked a debate in the literature on the use of regularization as a legitimate method, as successful works [36] were being published in spite of rising concerns. In 1996, Martin and Rizzo asserted that the subtraction of a linear state may remove log-singular terms without justification [60] and that $C^{0,\alpha}$ continuous elements could not be safely used with the simple solutions method.

In 1997, Richardson, Cruse, and Huang wrote a rebuttal to these concerns by analytically demonstrating the cancellation of singular terms by subtracting the linear state (i.e. EQ. (4.8)) [74]. Richardson et al. evaluated a general form Hadamard integral and demonstrated that log singular terms did exist in the integration, but would effectively sum to zero. Despite this, concerns were still given in further works [70].

Some authors have drawn conclusions on regularization and the simple solutions method based on both unsuccessful attempts to use the method, and also the criticisms mentioned before. One example is [70] which attempted to use the simple solutions method in conjunction with singular boundary conditions. However, this violated the restrictions outlined by Cruse and Richardson in [13, 74]. While that is a limitation of the method, it certainly is not representative of an overwhelming class of problems, and this limitation was discussed specifically in [74]. Primarily, it is suspected that the initial criticisms of

this method spawned from many authors using this technique with constant, linear, or quadratic, isoparametric elements and achieving poor results.

In [71], Richardson demonstrated something quite important that may have been overlooked by many during the debate over regularization that spanned the 1990s. Richardson demonstrated that by subtracting the linear state off of an interpolation function, the degree of that function was effectively reduced by two. A figure has been included here from that work [71] in Figure 4.1.

In reviewing Figure 4.1, it is seen that, for the case of a flat element, the behavior of a regularized quadratic function is effectively reduced to a constant across local elements. This means that codes using a two-term regularization in conjunction with a quadratic element were attempting to model complex densities with constants, and codes using linear elements were generating a null-density. Furthermore this figure helps cement the fact that not only are high order interpolations favorable, it shows that when combined with the simple solutions method high order interpolations *must* be used. One documented example is He, who obtained questionable results [31] when employing the simple solutions strategy. He employed the simple solutions strategy with quadratic elements, and it is certainly reasonable to suggest that his questionable results may have been a result of this. It is conceivable, perhaps probable, that many failed attempts with regularization were based on users attempting to model integrands with quadratic elements, resulting in a constant integrand. Specifically, the questionable results mentioned in [60] may have been linked to this issue.

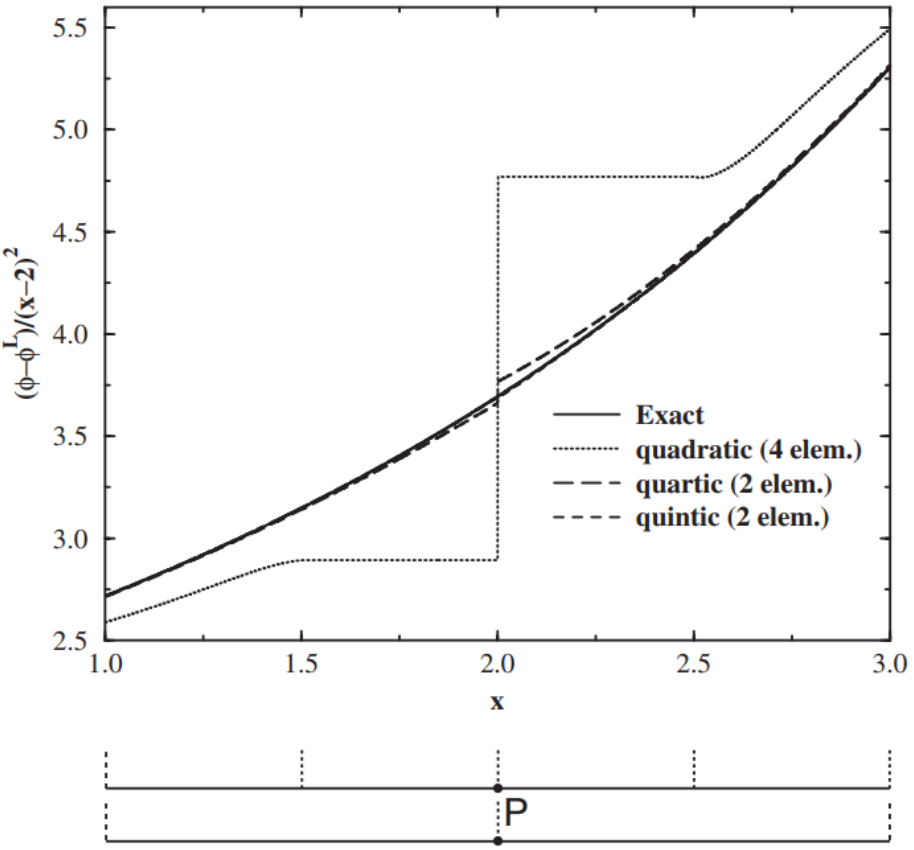

Figure 4.1

Polynomial refinement for the regularized integrand for $\phi(x) = e^x$. This figure originated from [71] and copyright has been obtained from John Wiley and Sons for its use here.

This work will present results of a p-version BEM, using the simple solutions method on both flat and curved geometries, to demonstrate its effectiveness. The examples in this study will target the case of steady-state heat transfer in three dimensions.

4.4 Numerical Implementation

This section will cover the necessary steps required to employ the simple solutions method, and also discuss the techniques employed by the computer code supporting this work.

4.4.1 Gaussian Quadrature

Gaussian quadrature is a popular quadrature rule based upon roots of the Gauss-Legendre polynomial. For the present case, standard square Gauss patterns were transformed in accordance with a standard Duffy transformation, such that the quadrature rules were suitable for weakly singular integrals. Chapter II discusses this transformation in detail. This is a standard quadrature approach.

Because the efficiency study in the present work requires refinement of the mesh, dense quadrature patterns (100x100) were chosen such that cases with more elements would not have an advantage from higher quadrature. The placement of nodes along the element were categorized into three cases: corner, edge, and interior. Each case has its own subdivision technique, which is given in Figure 4.2

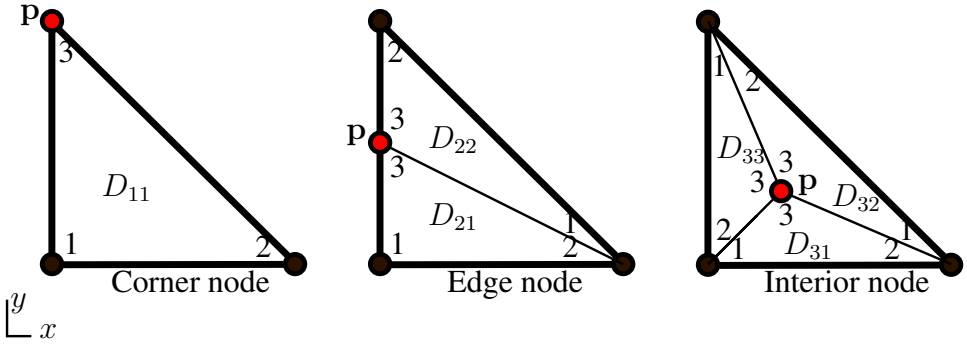

Figure 4.2

Depending on the location of P relative to the element surface, the domain of the element is to be subdivided. There are three cases for subdivision used here: corner, edge, and interior.

4.4.2 Interpolation Functions

The present work uses Lagrangian shape functions developed over triangular elements for its interpolation functions. The terms shape function and interpolation function are often used interchangeably in the context of numerical integration. The interpolation nodes were placed on a uniform grid across a unit triangular domain, and interpolation (shape) functions were generated in accordance with the Pascal triangle [100]. Symbolic computation packages (such as MATLAB, Maxima) can be used to achieve this. These interpolations represent a set of $C^{0,\alpha}$ continuous elements. This is important to note, as the use of these elements in this manner was a primary matter of the debate mentioned in Section 4.3.4.

The interpolation functions are developed in accordance with the value of the density at each of its nodes. In this case, the interpolations used for the density were also used for

geometry. Each interpolation can be seen as the dot product of the interpolation functions at the nodal locations, and the density at the nodal locations. When the density is not known at a node (case of unknown boundary conditions), these unknown terms will be placed in a vector of unknowns, $\{\mathbf{X}\}$, in the final system of equations. The interpolations are given in the form,

$$\begin{aligned} \phi(\mathbf{Q}) &\approx \sum_{k=1}^{\text{NPE}} N_k(\xi,\eta)\phi(\mathbf{Q})_k, \\ \frac{\mathrm{d}\phi(\mathbf{Q})}{\mathrm{d}\hat{n}} &\approx \sum_{k=1}^{\text{NPE}} N_k(\xi,\eta)\frac{\mathrm{d}\phi(\mathbf{Q})}{\mathrm{d}\hat{n}}\bigg|_k, \\ x &\approx \sum_{k=1}^{\text{NPE}} N_k(\xi,\eta)x_k \text{ (geometry)}, \end{aligned} \tag{4.11}$$

where

- NPE represents a potential function in three-dimensions,
- N represents the shape functions associated with local node k,
- $\psi(\mathbf{P},\mathbf{Q})$ is the Green's function in three dimensions (also known as the fundamental solution),
- and $\mathbf{P}$ and $\mathbf{Q}$ are the source and field points, respectively.

4.4.3 Green's Third Identity

To represent EQ. (4.10) in numerical form, the domain must be subdivided in accordance with its elements, and the shape functions must be evaluated over each integral with Gaussian quadrature. This results in the following numerical form,

$$\begin{aligned} 0 \approx \sum_{j=1}^{\text{NE}}\sum_{k=1}^{\text{NGP}} \Bigg[\Bigg(\sum_{n=1}^{\text{NPE}} N_n(\xi_k,\eta_k) \Bigg(-\frac{\mathrm{d}\psi(\mathbf{P},\mathbf{Q})}{\mathrm{d}\hat{n}(\mathbf{P})}\bigg|_n \frac{\mathrm{d}\left(\phi(\mathbf{Q})-\phi^L(\mathbf{Q})\right)}{\mathrm{d}\hat{n}(\mathbf{Q})}\bigg|_n \cdots \\ + \left(\phi(\mathbf{Q})-\phi^L(\mathbf{Q})\right)\frac{\mathrm{d}\psi(\mathbf{P},\mathbf{Q})}{\mathrm{d}\hat{n}(\mathbf{P})\mathrm{d}\hat{n}(\mathbf{Q})}\bigg|_n \Bigg)\Bigg)_k J(\xi_k,\eta_k)W_k \Bigg]_j \end{aligned} \tag{4.12}$$

where

- NE represents the number of elements,
- NGP represents the number of Gaussian quadrature points,
- $J(\xi, \eta)$ represents the Jacobian of the transformation,
- and W represents the weights of the Gaussian quadrature rule.

With the exception of the $\phi(\mathbf{Q})$ terms and the $\dfrac{\mathrm{d}\,\phi(\mathbf{Q})}{\mathrm{d}\hat{n}(\mathbf{Q})}$ terms, all terms in EQ. (4.12) can be directly evaluated and treated as constants. These constants are to be added together and stored in the form of a linear system.

In order to evaluate the Jacobian of the transformation, the intrinsic derivatives from EQ. (4.13) must be obtained. These are obtained by differentiating the shape functions directly. A symbolic computation package is recommended to develop these derivatives. These derivatives are evaluated as,

$$\begin{aligned} x_{,\xi} &= \sum_{n=1}^{\mathrm{NPE}} (N_{,\xi})_n \, x_n \,; \quad x_{,\eta} = \sum_{n=1}^{\mathrm{NPE}} (N_{,\eta})_n \, x_n \\ y_{,\xi} &= \sum_{n=1}^{\mathrm{NPE}} (N_{,\xi})_n \, y_n \,; \quad y_{,\eta} = \sum_{n=1}^{\mathrm{NPE}} (N_{,\eta})_n \, y_n \\ z_{,\xi} &= \sum_{n=1}^{\mathrm{NPE}} (N_{,\xi})_n \, z_n \,; \quad z_{,\eta} = \sum_{n=1}^{\mathrm{NPE}} (N_{,\eta})_n \, z_n \end{aligned} \tag{4.13}$$

The Jacobian of the transformation can then be evaluated using these terms. The Jacobian of the transformation is given as,

$$\begin{aligned} J_1 &= y_{,\xi} z_{,\eta} - z_{,\xi} y_{,\eta} \\ J_2 &= z_{,\xi} x_{,\eta} - x_{,\xi} z_{,\eta} \\ J_3 &= x_{,\xi} y_{,\eta} - y_{,\xi} x_{,\eta} \\ J &= \sqrt{J_1^2 + J_2^2 + J_3^2}. \end{aligned} \tag{4.14}$$

The surface normal can also be obtained,

$$\begin{aligned} n_x &= {}^{J_1}/_{J} \\ n_y &= {}^{J_2}/_{J} \\ n_z &= {}^{J_3}/_{J}. \end{aligned} \tag{4.15}$$

where $n_x,\ n_y,$ and n_z are components of the surface normal vector at the point $(\mathbf{Q})$. This normal can also be evaluated and point $(\mathbf{P})$ in the same manner. The construction of the final linear system is given in Section 4.4.4.

4.4.4 Implementation of Simple Solutions

In order to continue with the simple solutions method, the two term Taylor series centered at the singular point $(\mathbf{P} = \mathbf{Q})$ must be subtracted from EQ. (4.12). The Taylor series is given as,

$$\begin{aligned} \phi(\mathbf{Q})^L &= \phi(\mathbf{P}) + \vec{\nabla}\phi(\mathbf{P}) \cdot \vec{r}(\mathbf{P}, \mathbf{Q}) \\ \vec{\nabla}\phi(\mathbf{Q})^L &= \vec{\nabla}\phi(\mathbf{P}). \end{aligned} \tag{4.16}$$

The gradient is in Cartesian coordinates and is given as,

$$\vec{\nabla}\phi(\mathbf{P}) = \phi_{,x}(\mathbf{P})\hat{\mathbf{i}} + \phi_{,y}(\mathbf{P})\hat{\mathbf{j}} + \phi_{,z}(\mathbf{P})\hat{\mathbf{k}}. \tag{4.17}$$

The position, or distance vector, is in Cartesian coordinates and is given as,

$$\begin{aligned} \vec{r}(\mathbf{P}, \mathbf{Q}) &= (X_Q - X_P)\hat{\mathbf{i}} + (Y_Q - Y_P)\hat{\mathbf{j}} + (Z_Q - Z_Q)\hat{\mathbf{k}} \\ &= r_x\hat{\mathbf{i}} + r_y\hat{\mathbf{j}} + r_z\hat{\mathbf{k}} \end{aligned} \tag{4.18}$$

Because the integration in EQ. (4.12) takes place in the (ξ, η) spaces, the terms from the gradient expression must be expressed in terms of the (ξ, η) coordinates. To do this, a

rotation matrix is required to transform from Cartesian to the (ξ, η) space. To obtain this, one may begin with the expression,

$$\begin{Bmatrix} \phi_{,\xi} \\ \phi_{,\eta} \\ {}^{\mathrm{d}\phi}/_{\mathrm{d}\hat{n}} \end{Bmatrix} = \begin{bmatrix} x_{,\xi} & y_{,\xi} & z_{,\xi} \\ x_{,\eta} & y_{,\eta} & z_{,\eta} \\ n_x & n_y & n_z \end{bmatrix} \begin{Bmatrix} \phi_{,x} \\ \phi_{,y} \\ \phi_{,z} \end{Bmatrix}. \tag{4.19}$$

The rotation matrix, $[\mathbf{R}]$, is then obtained by,

$$[\mathbf{R}] = \begin{bmatrix} x_{,\xi} & y_{,\xi} & z_{,\xi} \\ x_{,\eta} & y_{,\eta} & z_{,\eta} \\ n_x & n_y & n_z \end{bmatrix}^{-1} = \begin{bmatrix} R_{11} & R_{12} & R_{13} \\ R_{21} & R_{22} & R_{23} \\ R_{31} & R_{32} & R_{33}. \end{bmatrix}, \tag{4.20}$$

which gives the transformation

$$\begin{Bmatrix} \phi_{,x} \\ \phi_{,y} \\ \phi_{,z} \end{Bmatrix} = \begin{bmatrix} R_{11} & R_{12} & R_{13} \\ R_{21} & R_{22} & R_{23} \\ R_{31} & R_{32} & R_{33} \end{bmatrix} \begin{Bmatrix} \phi_{,\xi} \\ \phi_{,\eta} \\ \phi_{,n} \end{Bmatrix}. \tag{4.21}$$

Substituting this result into the gradient gives,

$$\begin{aligned} \vec{\nabla}\phi(\mathbf{P}) &= (R_{11}\phi_{,\xi}(\mathbf{P}) + R_{12}\phi_{,\eta}(\mathbf{P}) + R_{13}\phi_{,n}(\mathbf{P}))\,\hat{\mathbf{i}} \\ &= (R_{21}\phi_{,\xi}(\mathbf{P}) + R_{22}\phi_{,\eta}(\mathbf{P}) + R_{23}\phi_{,n}(\mathbf{P}))\,\hat{\mathbf{j}} \\ &= (R_{31}\phi_{,\xi}(\mathbf{P}) + R_{32}\phi_{,\eta}(\mathbf{P}) + R_{33}\phi_{,n}(\mathbf{P}))\,\hat{\mathbf{k}}. \end{aligned} \tag{4.22}$$

It should be noted that $\phi_{,\xi}$ and $\phi_{,\eta}$ can be obtained from EQ. (4.13). The term $\phi_{,n}(\mathbf{P})$ is the same as $\dfrac{\mathrm{d}\phi(\mathbf{P})}{\mathrm{d}\hat{n}(\mathbf{P})}$, which will either be represented as an unknown, or a boundary

condition. When this result is substituted into EQ. (4.12), it will be dotted with either the position vector, $\vec{r}(\mathbf{P},\mathbf{Q})$ or the normal vector $n(\mathbf{Q})$. Both results are provided here,

$$\begin{aligned}\vec{\nabla}\phi(\mathbf{P})\cdot\vec{r}(\mathbf{P},\mathbf{Q}) = (R_{11}r_x + R_{21}r_y + R_{31}r_z)\sum_{n=1}^{\text{NPE}} N_{n,\xi}\phi_n(\mathbf{P}) \\ + (R_{12}r_x + R_{22}r_y + R_{32}r_z)\sum_{n=1}^{\text{NPE}} N_{n,\eta}\phi_n(\mathbf{P}) \\ + (R_{13}r_x + R_{23}r_y + R_{33}r_z)\frac{\mathrm{d}\phi(\mathbf{P})}{\mathrm{d}\hat{n}(\mathbf{P})},\end{aligned} \tag{4.23}$$

$$\begin{aligned}\vec{\nabla}\phi(\mathbf{P})\cdot\hat{n}(\mathbf{Q}) = (R_{11}n_x(\mathbf{Q}) + R_{21}n_y(\mathbf{Q}) + R_{31}n_z(\mathbf{Q}))\sum_{n=1}^{\text{NPE}} N_{,\xi}\phi_n(\mathbf{Q}) \\ + (R_{12}n_x(\mathbf{Q}) + R_{22}n_y(\mathbf{Q}) + R_{32}n_z(\mathbf{Q}))\sum_{n=1}^{\text{NPE}} N_{,\eta}\phi_n(\mathbf{Q}) \\ + (R_{13}n_x(\mathbf{Q}) + R_{23}n_y(\mathbf{Q}) + R_{33}n_z(\mathbf{Q}))\frac{\mathrm{d}\phi(\mathbf{P})}{\mathrm{d}\hat{n}(\mathbf{P})}.\end{aligned} \tag{4.24}$$

It is critical to note that the $\phi(\mathbf{Q})$ terms in the equations above represent terms associated with the *local* element. The relaxed regularization strategy discussed in [74] requires that only the local approximation for the gradient is subtracted on each element. The gradient must also be integrated over the entire body. For the distant elements, an average approximation for the linear state on all local elements is used in the integrals. For example, if a node were to be shared by four elements, local elements would use the expression for the gradient obtained from *that* element, and far field elements would use an averaged expression of the gradients from each local element.

Each time the gradient is evaluated, it will result in a vector of constants dotted with all ϕ terms on local elements, and will also result in a single constant times $\frac{\mathrm{d}\phi(\mathbf{P})}{\mathrm{d}\hat{n}(\mathbf{P})}$. These terms will be used in conjunction with EQ. (4.12) to construct the linear system.

4.4.5 Linear System

Once the terms from EQs. (4.12), (4.23), and (4.24), are obtained, two matrices of coefficients can be created. The matrices can be written as,

$$[\mathbf{A}]\left\{{}^{\mathrm{d}\phi}/_{\mathrm{d}\hat{n}}\right\} + [\mathbf{B}]\{\phi\} = \{0\}\,, \tag{4.25}$$

where the column vectors $\left\{{}^{\mathrm{d}\phi}/_{\mathrm{d}\hat{n}}\right\}$ and $\{\phi\}$ represent the nodal values of ϕ and ${}^{\mathrm{d}\phi}/_{\mathrm{d}\hat{n}}$ in association with the boundary mesh. It should be noted that the right hand side becomes zero from the regularization. Depending on boundary conditions, certain terms of these column vectors will be known, and can be moved to the right hand side. In the present case, routines from LAPACK were used to solve the final system of equations [2].

4.5 Modelling of Geometries

Two cases of geometry were used to obtain the results herein. The first represents a mesh of a cube with no modelling error other than round-off, and the second represents a mesh of a sphere with an unknown degree of modelling error.

4.5.1 Discretization of a Cube

Due to lack of support for high order interpolations in modern meshing software libraries, an external algorithm was used to convert linear meshes into high order meshes. The reference meshes used were triangular meshes with nodes spaced at uniform grid locations. The density of the grid increases with the element order. An initial cube mesh was generated from Delaunay Triangulation, and then obtaining the convex hull of that triangulation.

The first case is a unit cube centered at (0,0,0) with corners placed at $(\pm 1, \pm 1, \pm 1)$. The unit cube represents a nearly perfect geometry which should have no modelling error from integration, other than finite precision. It is noted that the edges and corners of cubes create sites to accumulate error [75]. Boundary conditions were chosen such that flux was known on every surface but the positive z face. It is further noted that corners may have a high number of unknown fluxes, one for each face. A further study of this would be reserved for future work.

The cubes used in the present study range from 12 to 300 elements to give a variety of system sizes.

4.5.2 Discretization of a Sphere

The second case in example is an eight element spherical mesh, centered at (0,0,0), with a radius of one. The spherical mesh is a research mesh and should represent a significant modelling challenge, as interpolations will not be able to capture the surface perfectly. Furthermore, the locations of the surface nodes were obtained through a hybrid stochastic and gradient based optimization developed by J.D. Richardson. The spherical surface is also curved and will exhibit complex Jacobians of transformation, increasing the difficulty of numerical integration. The sphere has an unknown degree of modelling error, and is considered an excellent candidate to represent the method's effectiveness on a numerically challenging surface. The mesh is visualized in Figure (4.11).

4.6 Numerical Examples

The examples in this work represent cases of steady-state heat transfer with mixed boundary conditions.

4.6.1 Steady State Heat Transfer on the Unit Cube: h-p Convergence (Example 1)

The first experiment is the modeling of a transcendental function which cannot be perfectly modelled by polynomials. Additionally, cubes are used such that no significant modelling error is introduced. Boundary conditions are such that all surfaces are Neumann ($^{d\phi}/_{d\hat{n}}$ is known), except for the $+z$ surface, which is Dirichlet (ϕ is known). Multiple meshes are used for this experiment, with refinements ranging from 12 elements to 300 elements, as shown in Figures 4.3 and 4.4. Further discussion of the meshes can be found in Section 4.5.1.

Boundary conditions are in accordance with the function,

$$\phi = 10e^{0.3x}\sin(0.3y) + 10e^{0.3y}\sin(0.3z) + 10e^{0.3z}\sin(0.3x). \tag{4.26}$$

Error is based on normalized errors located at corners and is given by

$$\text{ErrorNorm} = \frac{\sum(\text{Error at corners})}{\text{Largest observed surface value}} \tag{4.27}$$

In this experiment, both element number (increasing number of elements) and element order (increasing interpolation order) were refined and trends were observed. Curves depicting h-p convergence are demonstrated in Figure (4.5). Figure 4.5 shows clear computational advantage when using high order interpolations. The increase in accuracy can be observed by trends in the figure. For example, one can hold system size constant at 386,

and gain three orders of magnitude in accuracy by choosing the octic interpolation over the quartic. Furthermore, it is seen that a septic element at a system size of 296 will offer the same effective accuracy of a quartic element at a system size of 1538.

It has been shown that quartic elements in conjunction with the simple solutions method are comparable to quadratic elements from other hypersingular BEM algorithms [73]. This is due to the fact that regularization sacrifices low order interpolation degrees of freedom. Therefore, one may consider the quartic curve in this figure similar to quadratic elements in the BEM [71].

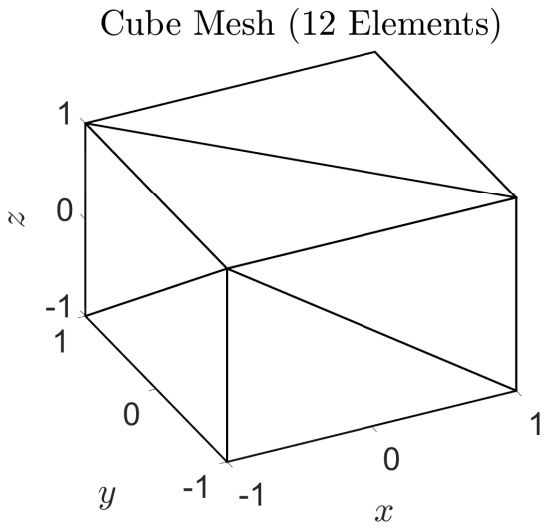

Boundary Conditions		
Surface	Known	Unknown
$+x$	$d\phi/d\hat{n}$	ϕ
$-x$	$d\phi/d\hat{n}$	ϕ
$+y$	$d\phi/d\hat{n}$	ϕ
$-y$	$d\phi/d\hat{n}$	ϕ
$+z$	ϕ	$d\phi/d\hat{n}$
$-z$	$d\phi/d\hat{n}$	ϕ

Figure 4.3

Representation of one of the meshes used to generate results for Examples 1 and 2.

Shown is a unit cube discretized into 12 elements.

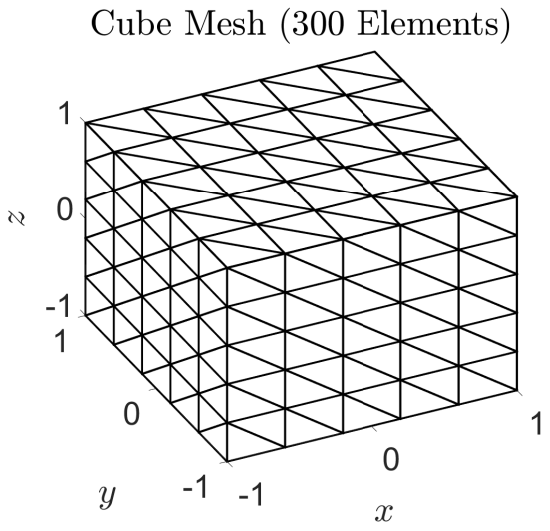

Boundary Conditions		
Surface	Known	Unknown
$+x$	$d\phi/d\hat{n}$	ϕ
$-x$	$d\phi/d\hat{n}$	ϕ
$+y$	$d\phi/d\hat{n}$	ϕ
$-y$	$d\phi/d\hat{n}$	ϕ
$+z$	ϕ	$d\phi/d\hat{n}$
$-z$	$d\phi/d\hat{n}$	ϕ

Figure 4.4

Representation of one of the meshes used to generate results for Example 1. Shown is a unit cube discretized into 300 elements.

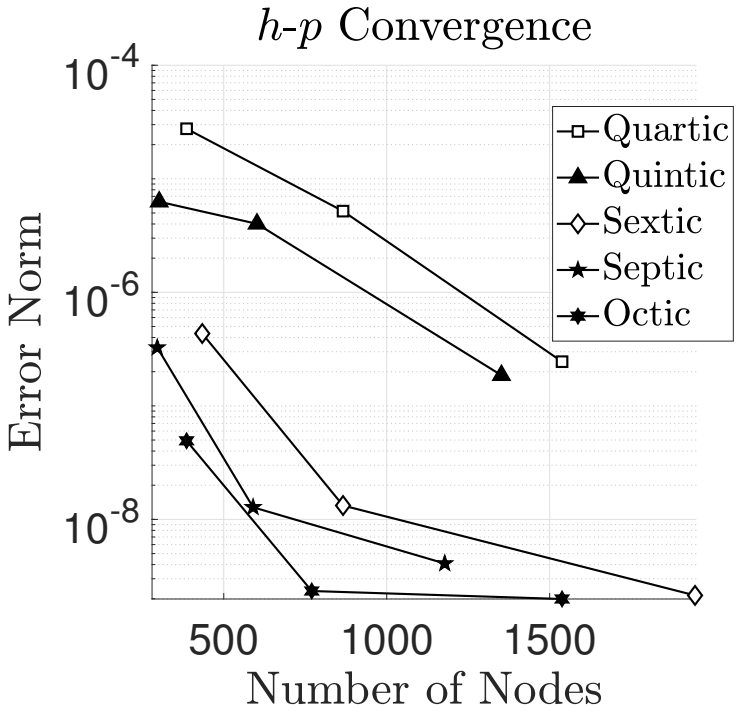

Figure 4.5

Convergence of various interpolation orders are observed for EQ. (4.26). (Example 1)

4.6.2 Steady State Heat Transfer on the Unit Cube: Increased Spatial Frequency (Example 2)

The second experiment is the modeling of a transcendental function, with increased spatial frequency, which also cannot be perfectly modelled by polynomials. Additionally, the cube is used such that no significant modelling error is introduced. Boundary conditions are such that all surfaces are Neumann (${}^{\mathrm{d}\phi}/_{d\hat{n}}$ is known), except for the $+z$ surface, which is Dirichlet (ϕ is known). The mesh used for this experiment is shown in Figure (4.3), which is a twelve element mesh. Further discussion of the mesh can be found in Section 4.5.1.

Boundary conditions are in accordance with the function,

$$\phi = 10e^{3x}\sin(3y) + 10e^{3y}\sin(3z) + 10e^{3z}\sin(3x). \tag{4.28}$$

Absolute error is based on a nodal basis and is given by,

$$\text{ABS Error} = |\text{Numerical approximation} - \text{True solution}|. \tag{4.29}$$

The errors shown in Figures 4.7 through 4.9 are based on the normalized error given by

$$\text{ErrorNorm} = \frac{\text{ABS Error}}{\text{Largest observed surface value}} \tag{4.30}$$

In this experiment, three element interpolations (octic, decic, duodecic) are used to attempt to capture ϕ, and the results are investigated for each. First, approximations are investigated over the edge $(x = 1, y, z = -1)$, which is an edge where errors are shown to accumulate. Approximations for this edge are compared against the true solution and shown in Figure 4.6. Figure 4.6 shows increased interpolation orders capturing the true solution.

Errors are also investigated over the positive x face of the unit cube domain. Figures 4.7 through 4.10 demonstrate the ability for an increase in interpolation to capture a numerically challenging potential, and allow the reader to visualize both the accuracy of the method, and the location of errors. Errors shown are the absolute difference in the true solution, and the numerical approximation. Provided are results for octic, decic, and duodecic elements. It should be noted that octic elements show normalized errors on the order of 10^{-1}, where duodecic elements show errors on the order of 10^{-5}.

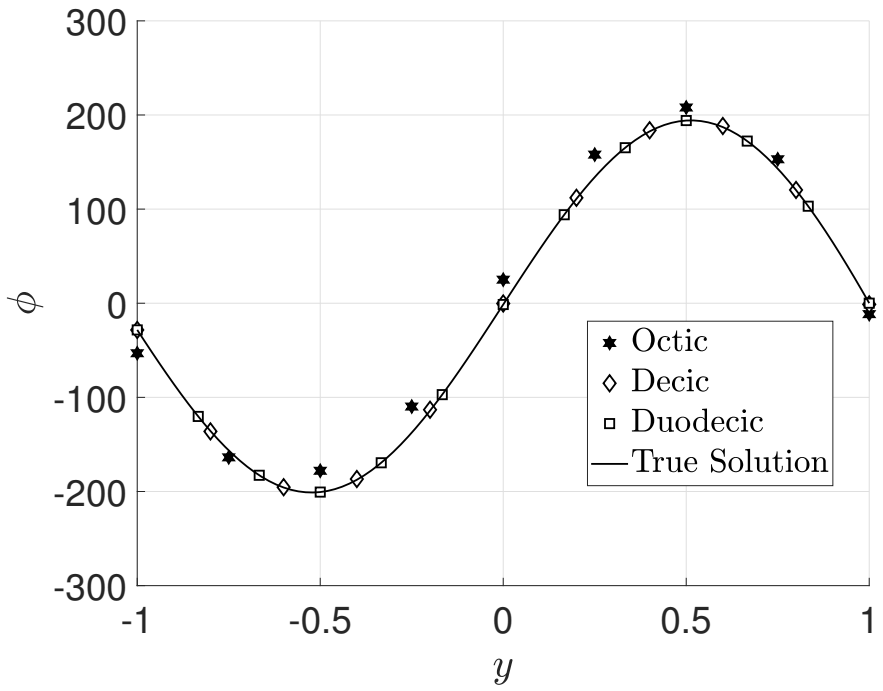

Figure 4.6

Fitting of numerical approximations to ϕ across the cube edge $(x = 1, y, z = -1)$ are shown here. (Example 2)

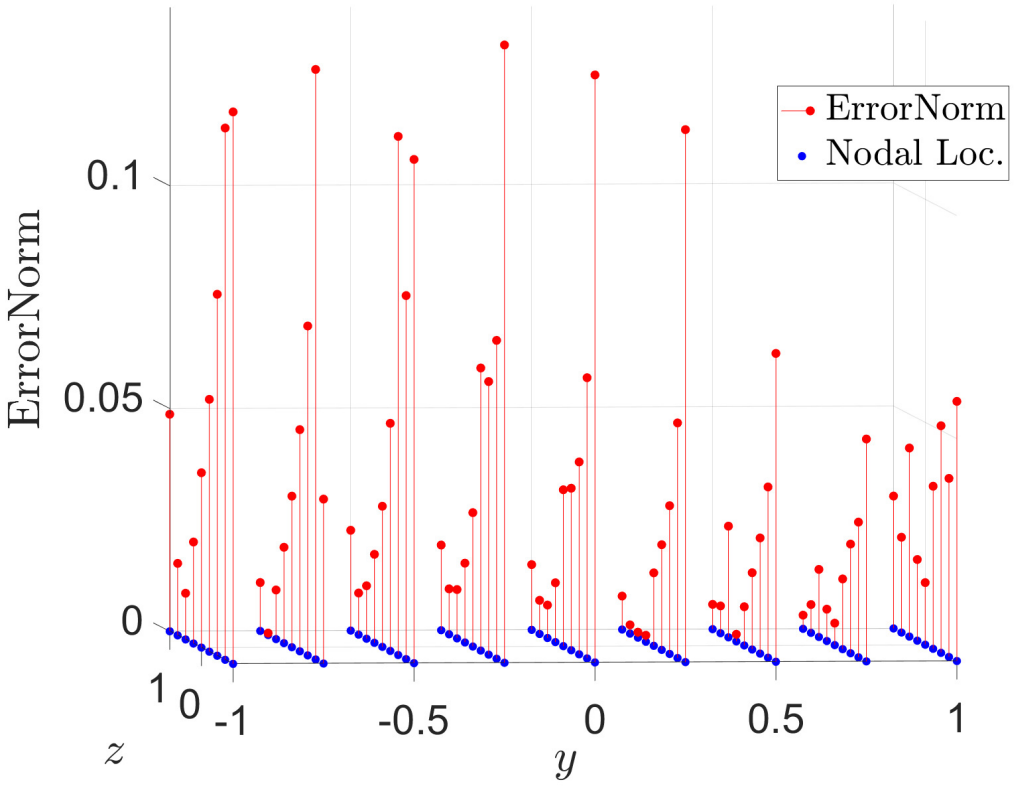

Figure 4.7

Distribution of normalized errors for octic interpolations along the positive x face of the unit cube. (Example 2)

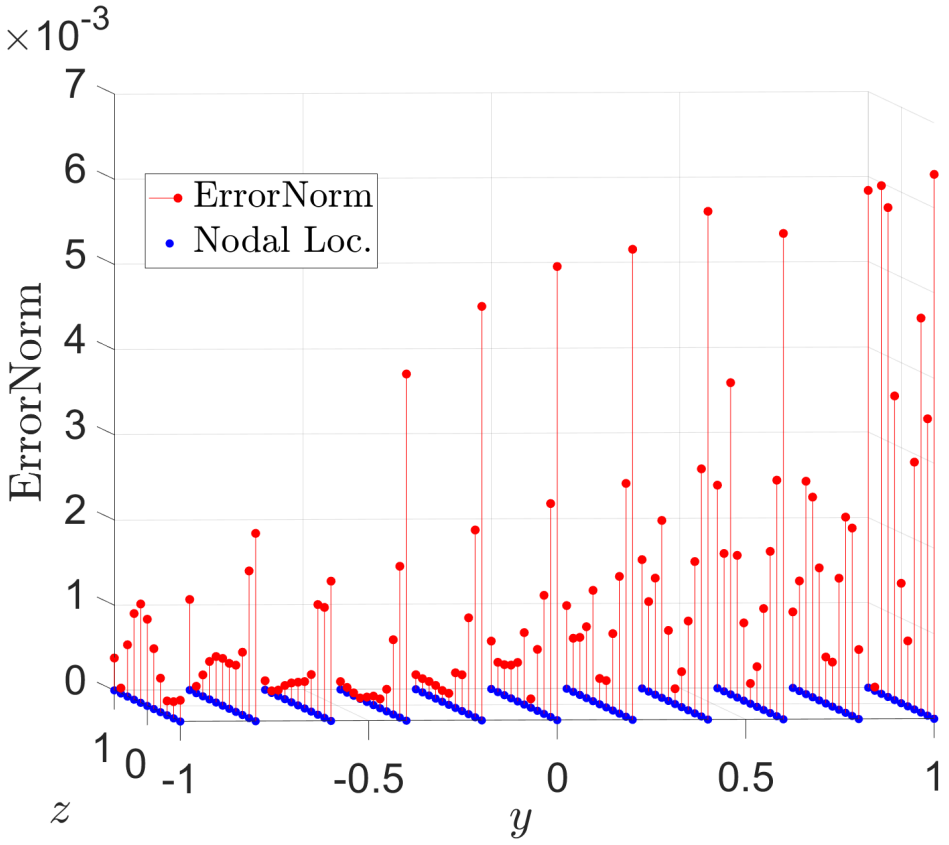

Figure 4.8

Distribution of normalized errors for decic interpolations along the positive x face of the unit cube. (Example 2)

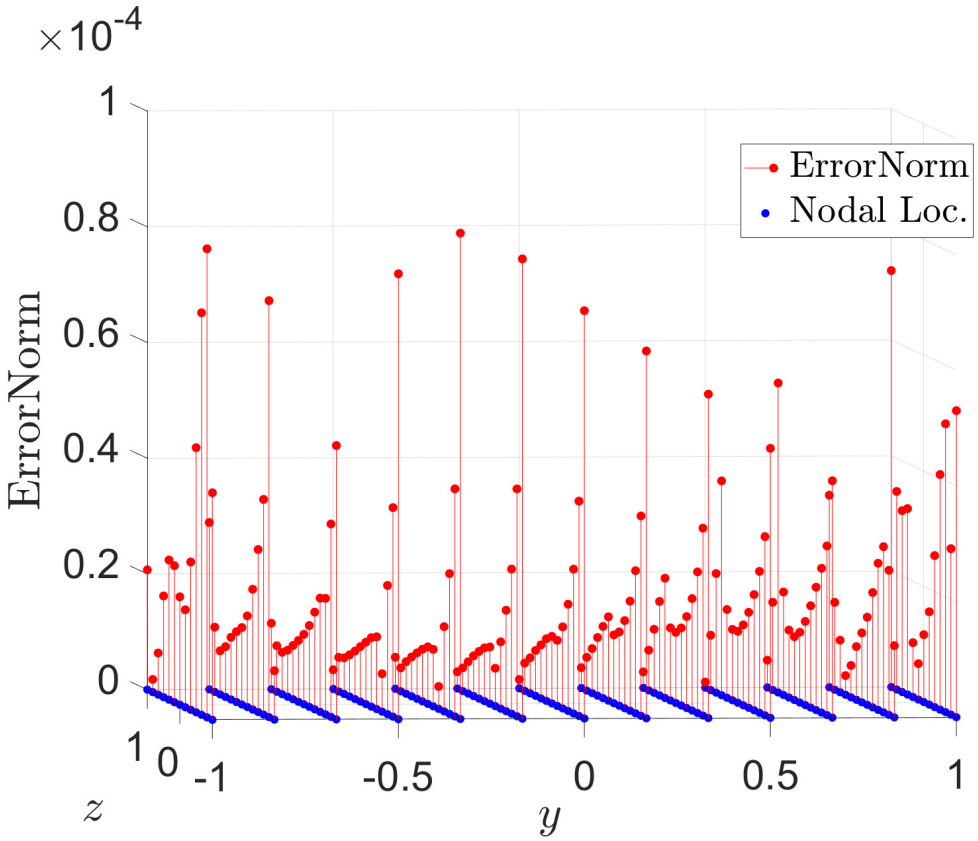

Figure 4.9

Distribution of normalized errors for duodecic interpolations along the positive x face of the unit cube. (Example 2)

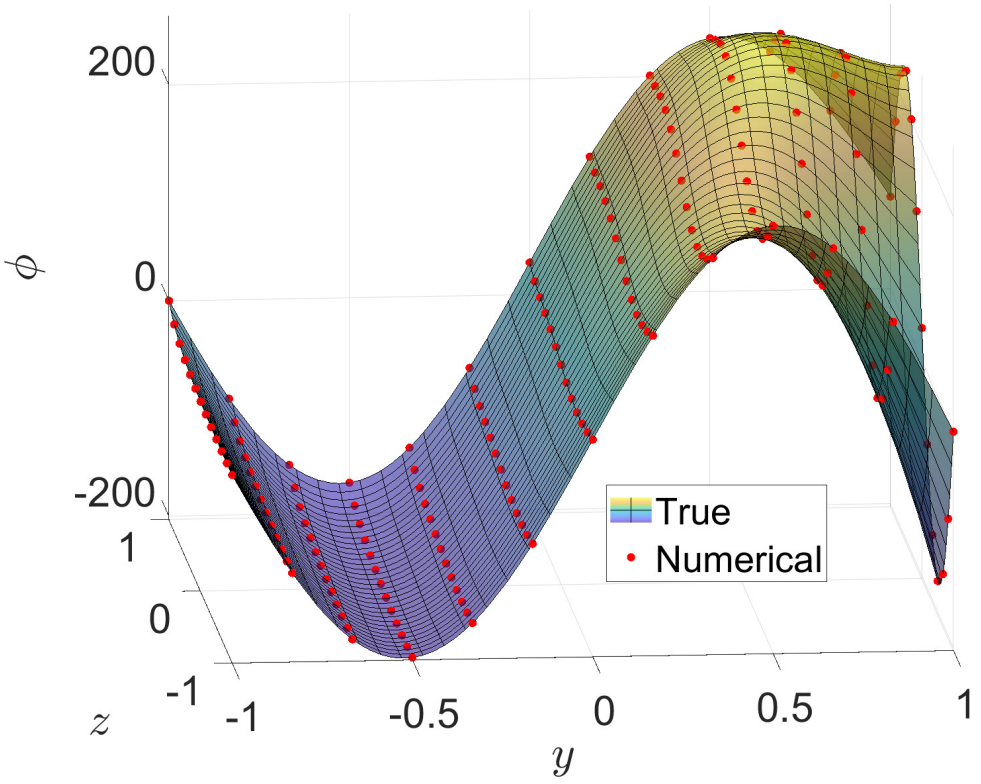

Figure 4.10

Fitting of numerical approximations (duodecic elements) to ϕ across the positive x face of the unit cube. (Example 2)

4.6.3 Steady State Heat Transfer on the Unit Sphere: Curved, General Surfaces (Example 3)

The third experiment is the modeling of a transcendental function which cannot be perfectly modelled by polynomials. The modeling error in the sphere is unknown, and the geometry cannot be exactly modelled with finite order interpolations. Boundary conditions are such that the $+z$ half of the sphere is Dirichlet and the $-z$ portion is Neumann. This case exhibits significant elemental distortion through curved surfaces and complex Jacobians. Additionally, normals are discontinuous at element junctions, exhibiting differences on the order of 10^{-5}, but are averaged to a single estimated value. This case is chosen to represent a general surface problem. The mesh used for this experiment is an eight element mesh and is shown in Figure (4.11). Further discussion of this mesh can be found in Section 4.5.2.

Boundary conditions are in accordance with the function,

$$\phi = 10e^{0.3x}\sin(0.3y) + 10e^{0.3y}\sin(0.3z) + 10e^{0.3z}\sin(0.3x). \tag{4.31}$$

This case was run with octic elements on the unit sphere discretized into eight elements. To represent a practical case, a 30x30 Duffy quadrature rule was used locally, with a 1200 point rule for far field elements.

Approximations were observed over the edge $(r = 1, \theta, z = 0)$ and compared against the true solution in Figure 4.12. In addition, tabular results are provided in Table 4.1. Errors shown are normalized errors according to EQ. (4.30). These results show that the method is capable of delivering engineering accuracies on imperfect, general surfaces in a short

amount of time. This simulation was ran on an ACER Aspire V 15 laptop (i7 processor, 8GB DDR3 L Memory, LINUX environment), and obtained a run time 5.75 seconds.

Table 4.1

Results of interest for the unit sphere. (Example 3)

Unit Sphere Results		
Result	ϕ	$\mathrm{d}\phi/\mathrm{d}\hat{n}$
Maximum Normalized Error	$1.37(10^{-4})$	$1.69(10^{-4})$
Minimum Normalized Error	$4.98(10^{-7})$	$3.22(10^{-8})$
Run Time	5.75 seconds	-
System Size	258x258	-

4.7 Conclusions

This work investigated the use of the simple solutions technique applied to the gradient of Green's third identity in the context of the boundary element method. The method has received criticism in the past, some authors reporting poor or mediocre results. History shows that previous authors may have missed the fact that orders of interpolation are effectively lost when using the simple solutions technique. Previous authors have reported success in the past, showing elemental efficiency for a p-version BEM in two dimensions [71], and it was desired to extend this advantage to three dimensions.

The results of this work show that by regularizing hypersingular integrals with the simple solutions technique, the BEM can easily and readily support high order elements.

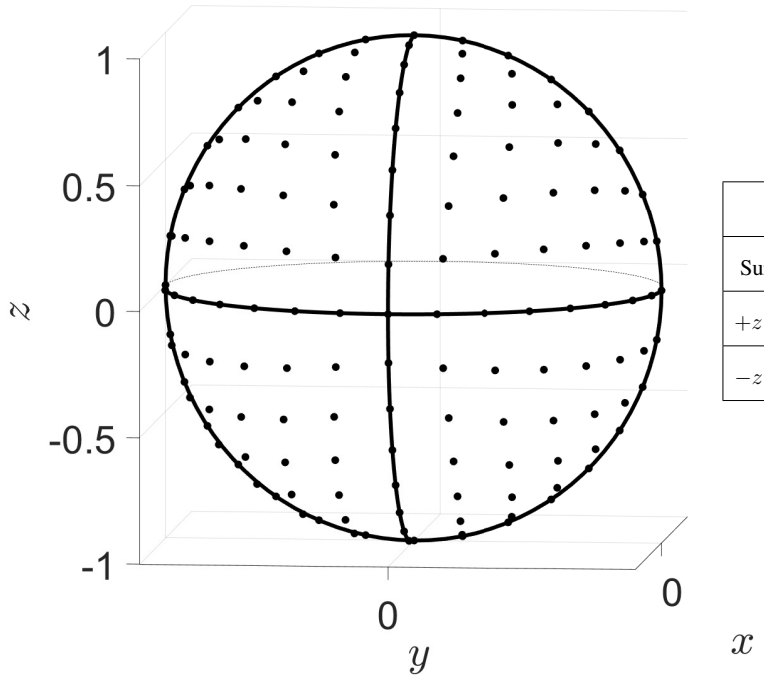

Boundary Conditions		
Surface	Known	Unknown
$+z$	ϕ	$\mathrm{d}\phi/\mathrm{d}\hat{n}$
$-z$	$\mathrm{d}\phi/\mathrm{d}\hat{n}$	ϕ

Figure 4.11

Shown is a unit sphere discretized into eight curved elements, representing octic interpolations. This mesh represents a research mesh. Nodal locations were obtained using a mesh optimization algorithm generated by J.D. Richardson. (Example 3)

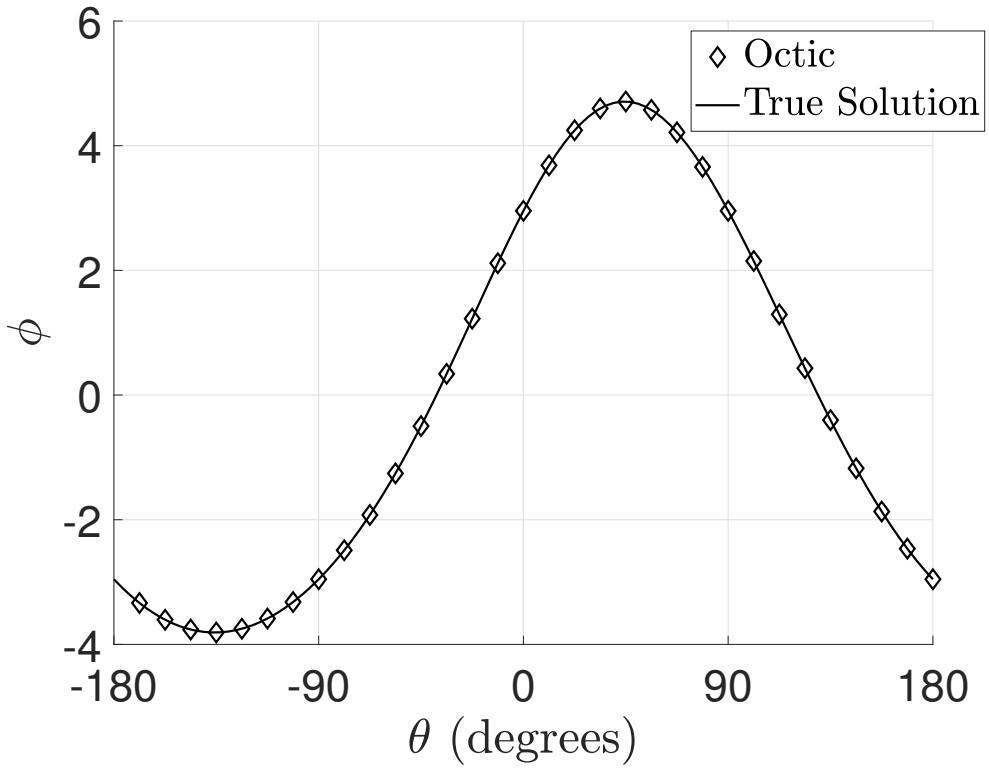

Figure 4.12

Numerical solution for ϕ across the edge $(r = 1, \theta, z = 0)$ of the unit sphere. (Example 3)

Many works in the literature rely on closed form techniques to address the problem of the hypersingular integral in the BEM. However, closed form techniques are often too tedious to allow the study of different element types. The present treatment allows for direct numerical integration, and thus no barriers preventing the support of high interpolations are present.

Results show that the use of high order elements (quartic through octic) will result in significant computational efficiency, reducing errors by three orders of magnitude for a constant system size, or reducing system size by three orders of magnitude for the same accuracy. This is consistent with the convergence seen by Richardson [71] in two dimensions. Additionally, it was shown that the simple solutions method can prove effective on approximate meshes on curved geometries, while still obtaining results suitable for engineering accuracy.

CHAPTER V

CONCLUSIONS

This work provided several contributions to the area of numerical integration for boundary integral methods, primarily targeting the boundary element method.

The first work was an improvement to numerical integration of near hypersingular integrals. Near hypersingular integrals appear in certain boundary integral formulations. Specifically, the method of functional equations as described by Kupradze, and also for thin-body problems. The method presented uses an elemental distortion to shift quadrature locations toward the singularity, improving stacking in the radial direction. Errors show that the method is competitive with modern techniques, and can also offer quadrature reductions of 75 percent over the standard Duffy method.

The second work was an improvement to integration of weakly singular integrals. This work showed that by using regularization, weakly singular integrals can be separated into two parts. One part may be integrated in closed form, while the other is effectively smoothed and much more amenable to numerical integration. Errors show that the method may easily reduce errors by several orders of magnitude for the same quadrature order.

The final work investigated the use of regularization (the simple solutions technique) applied to hypersingular integrals in the context of the boundary element method. Many

previous works have debated over this method, citing poor results, concerns in continuity requirements, and removing singular terms without justification. This work showed that by using the simple solutions technique, the BEM can be reduced to a weakly singular form which directly supports numerical integration. Additionally, the technique completely removes the need for closed form integration, and allows for the support of high order interpolations. The work showed that the p-version BEM can offer increases in computational efficiency by several orders of magnitude in terms of error and system size. Results support that the method is accurate and effective. This work may serve as a baseline study for the p-version BEM in three dimensions, paving the way for future convergence studies in new areas of application for the simple solutions method.

REFERENCES

[1] M. H. Aliabadi, *The boundary element method, applications in solids and structures*, vol. 2, John Wiley & Sons, 2002.

[2] E. Anderson, Z. Bai, J. Dongarra, A. Greenbaum, A. McKenney, J. Du Croz, S. Hammarling, J. Demmel, C. Bischof, and D. Sorensen, "LAPACK: A portable linear algebra library for high-performance computers," *Proceedings of the 1990 ACM/IEEE conference on Supercomputing*. IEEE Computer Society Press, 1990, pp. 2–11.

[3] S. Arjunon, "p-version Refinement Studies in the Boundary Element Method," *Tennessee Technological University*, 2009.

[4] S. Arjunon and J. Richardson, "Regularized p-version collocation BEM algorithms for two-dimensional heat conduction," *Engineering analysis with boundary elements*, vol. 29, no. 10, 2005, pp. 953–962.

[5] P. K. Banerjee and R. Butterfield, *Boundary element methods in engineering science*, vol. 17, McGraw-Hill London, 1981.

[6] R. S. Barsoum, "Triangular quarter-point elements as elastic and perfectly-plastic crack tip elements," *International Journal for numerical Methods in engineering*, vol. 11, no. 1, 1977, pp. 85–98.

[7] A. A. Becker, *The Boundary Element Method in Engineering: A Complete Course*, Book. McGraw-Hill, New York City, NY, 1992.

[8] R. L. Burden, J. D. Faires, and A. Burden, *Numerical Analysis*, Cengage Learning, 2016.

[9] G. S. Chandekar, J. D. Richardson, Y. A. Melnikov, and S. J. Pardue, "Green's Function Method for an Axisymmetric Void Between Parallel Walls," *Electronic Journal of Boundary Elements*, vol. 5, no. 2, 2007.

[10] C.-S. Chen, A. Karageorghis, and Y. S. Smyrlis, *The Method of Fundamental Solutions: A Meshless Method*, Dynamic Publishers Atlanta, 2008.

[11] T. Cruse, "A direct formulation and numerical solution of the general transient elastodynamic problem. II," *Journal of Mathematical Analysis and Applications*, vol. 22, no. 2, 1968, pp. 341–355.

[12] T. Cruse, "Numerical solutions in three dimensional elastostatics," *International journal of solids and structures*, vol. 5, no. 12, 1969, pp. 1259–1274.

[13] T. Cruse and J. Richardson, "Non-Singular Somigliana Stress Identities in Elasticity," *International Journal for Numerical Methods in Engineering*, vol. 39, no. 19, 1996, pp. 3273–3304.

[14] T. Cruse and W. Vanburen, "Three-dimensional elastic stress analysis of a fracture specimen with an edge crack," *International Journal of Fracture Mechanics*, vol. 7, no. 1, 1971, pp. 1–15.

[15] T. A. Cruse, "Application of the boundary-integral equation method to three dimensional stress analysis," *Computers & Structures*, vol. 3, no. 3, 1973, pp. 509–527.

[16] T. A. Cruse, "An improved boundary-integral equation method for three dimensional elastic stress analysis," *Computers & Structures*, vol. 4, no. 4, 1974, pp. 741–754.

[17] T. A. Cruse and F. J. Rizzo, "A direct formulation and numerical solution of the general transient elastodynamic problem. I," *Journal of Mathematical Analysis and Applications*, vol. 22, no. 1, 1968, pp. 244–259.

[18] A. Deb and P. Banerjee, "A comparison between isoparametric Lagrangian elements in 2D BEM," *International journal for numerical methods in engineering*, vol. 28, no. 7, 1989, pp. 1539–1555.

[19] M. G. Duffy, "Quadrature over a pyramid or cube of integrands with a singularity at a vertex," *SIAM journal on Numerical Analysis*, vol. 19, no. 6, 1982, pp. 1260–1262.

[20] G. Fairweather and A. Karageorghis, "The method of fundamental solutions for elliptic boundary value problems," *Advances in Computational Mathematics*, vol. 9, no. 1-2, 1998, p. 69.

[21] E. A. Galapon, "The Cauchy principal value and the Hadamard finite part integral as values of absolutely convergent integrals," *Journal of Mathematical Physics*, vol. 57, no. 3, 2016, p. 033502.

[22] L. Gray, "Symbolic computation of hypersingular boundary integrals," *Advances in boundary element techniques*, Springer, 1993, pp. 157–172.

[23] G. Green, *An essay on the application of mathematical analysis to the theories of electricity and magnetism*, Wezäta-Melins Aktiebolag, 1828.

[24] Y. Gu, W. Chen, and C. Zhang, "The sinh transformation for evaluating nearly singular boundary element integrals over high-order geometry elements," *Engineering Analysis with Boundary Elements*, vol. 37, no. 2, 2013, pp. 301–308.

[25] Y. Gu, W. Chen, and C. Zhang, "Stress analysis for thin multilayered coating systems using a sinh transformed boundary element method," *International Journal of Solids and Structures*, vol. 50, no. 20-21, 2013, pp. 3460–3471.

[26] Y. Gu, Q. Hua, W. Chen, and C. Zhang, "Numerical evaluation of nearly hypersingular integrals in the boundary element analysis," *Computers & Structures*, vol. 167, 2016, pp. 15–23.

[27] M. Guiggiani, "Computing principal-value integrals in 3-D BEM for time-harmonic elastodynamics–A direct approach," *Communications in applied numerical methods*, vol. 8, no. 3, 1992, pp. 141–149.

[28] M. Guiggiani and A. Gigante, "A general algorithm for multidimensional Cauchy principal value integrals in the boundary element method," *Journal of Applied Mechanics*, vol. 57, no. 4, 1990, pp. 906–915.

[29] A. Guz and V. Zozulya, "Brittle fracture of constructive materials under dynamic loading," *Naukova Dumka, Kiev*, 1993.

[30] J. Hadamard, *Lectures on Cauchy's problem in linear partial differential equations*, Courier Corporation, 1952.

[31] M. He and C. Tan, "A Self-regularization Technique in Boundary Element Method for 3-D Stress Analysis," *CMES: Computer Modeling in Engineering & Sciences*, vol. 95, no. 4, 2013, pp. 317–349.

[32] N. Heuer, M. E. Mellado, and E. P. Stephan, "A p-adaptive algorithm for the BEM with the hypersingular operator on the plane screen," *International journal for numerical methods in engineering*, vol. 53, no. 1, 2002, pp. 85–104.

[33] S. Holzer, "How to deal with hypersingular integrals in the symmetric BEM," *International Journal for Numerical Methods in Biomedical Engineering*, vol. 9, no. 3, 1993, pp. 219–232.

[34] S. M. Holzer, "The h-, p-and hp-versions of the BEM in elasticity: Numerical results," *Communications in numerical methods in engineering*, vol. 11, no. 3, 1995, pp. 255–265.

[35] Q. Huang and T. Cruse, "Some notes on singular integral techniques in boundary element analysis," *International journal for numerical methods in engineering*, vol. 36, no. 15, 1993, pp. 2643–2659.

[36] Q. Huang and T. Cruse, "On the non-singular traction-BIE in elasticity," *International Journal for Numerical Methods in Engineering*, vol. 37, no. 12, 1994, pp. 2041–2072.

[37] M. Hussain, W. Lorensen, and G. Pflegel, "The quarter-point quadratic isoparametric element as a singular element for crack problems," *nasa.gov*, 1976.

[38] M. Jaswon and A. Ponter, "An integral equation solution of the torsion problem," *Proceedings of the Royal Society of London. Series A. Mathematical and Physical Sciences*, vol. 273, no. 1353, 1963, pp. 237–246.

[39] B. M. Johnston and P. R. Johnston, "A comparison of transformation methods for evaluating two-dimensional weakly singular integrals," *International journal for numerical methods in engineering*, vol. 56, no. 4, 2003, pp. 589–607.

[40] B. M. Johnston, P. R. Johnston, and D. Elliott, "A sinh transformation for evaluating two-dimensional nearly singular boundary element integrals," *International journal for numerical methods in engineering*, vol. 69, no. 7, 2007, pp. 1460–1479.

[41] P. R. Johnston, "Application of sigmoidal transformations to weakly singular and near-singular boundary element integrals," *International journal for numerical methods in engineering*, vol. 45, no. 10, 1999, pp. 1333–1348.

[42] P. R. Johnston and D. Elliott, "A sinh transformation for evaluating nearly singular boundary element integrals," *International journal for numerical methods in engineering*, vol. 62, no. 4, 2005, pp. 564–578.

[43] P. R. Johnston, B. M. Johnston, and D. Elliott, "Using the iterated sinh transformation to evaluate two dimensional nearly singular boundary element integrals," *Engineering Analysis with Boundary Elements*, vol. 37, no. 4, 2013, pp. 708–718.

[44] L. Kantorovich, "On approximate calculation of some type of definite integrals and other applications of the method of singularities extraction," *Matematicheskii Sbornik*, vol. 41, no. 2, 1934, pp. 235–245.

[45] M. Katsurada and H. Okamoto, "The collocation points of the fundamental solution method for the potential problem," *Computers & Mathematics with Applications*, vol. 31, no. 1, 1996, pp. 123–137.

[46] O. D. Kellogg, *Foundations of potential theory*, vol. 31, Springer Science & Business Media, 2012.

[47] M. A. Khayat, D. R. Wilton, and P. W. Fink, "An improved transformation and optimized sampling scheme for the numerical evaluation of singular and near-singular potentials," *IEEE Antennas and Wireless Propagation Letters*, vol. 7, 2008, pp. 377–380.

[48] E. Kreyszig, "Advanced Engineering Mathematics, 8-th edition,", 1999.

[49] G. Krishnasamy, F. Rizzo, and T. Rudolphi, "Continuity requirements for density functions in the boundary integral equation method," *Computational Mechanics*, vol. 9, no. 4, 1992, pp. 267–284.

[50] V. Kupradze and M. A. Aleksidze, "The method of functional equations for the approximate solution of certain boundary value problems," *USSR Computational Mathematics and Mathematical Physics*, vol. 4, no. 4, 1964, pp. 82–126.

[51] V. D. Kupradze, *Potential methods in the theory of elasticity*, Israel program for scientific translations, 1965.

[52] X. Li and Y. Su, "Three-dimensional stress analysis of thin structures using a boundary element method with sinh transformation for nearly singular integrals," *Computers & Mathematics with Applications*, vol. 72, no. 11, 2016, pp. 2773–2787.

[53] Y. Liu, "Analysis of shell-like structures by the boundary element method based on 3-D elasticity: formulation and verification," *International Journal for Numerical Methods in Engineering*, vol. 41, no. 3, 1998, pp. 541–558.

[54] Y. Liu, "On the simple-solution method and non-singular nature of the BIE/BEMa review and some new results," *Engineering analysis with boundary elements*, vol. 24, no. 10, 2000, pp. 789–795.

[55] Y. Liu and F. Rizzo, "A weakly singular form of the hypersingular boundary integral equation applied to 3-D acoustic wave problems," *Computer Methods in Applied Mechanics and Engineering*, vol. 96, no. 2, 1992, pp. 271–287.

[56] E. Lutz, "Exact Gaussian quadrature methods for near-singular integrals in the boundary element method," *Engineering analysis with boundary elements*, vol. 9, no. 3, 1992, pp. 233–245.

[57] E. Lutz, L. Gray, and A. Ingraffea, "Indirect evaluation of surface stress in the boundary element method," *Boundary Integral Methods*, Springer, 1991, pp. 339–348.

[58] L. E. Malvern, *Introduction to the Mechanics of a Continuous Medium*, Number Monograph. Pearson, 1969.

[59] J. P. Marshall, J. D. Richardson, and C. J. Montalvo, "Greens function–based surrogate model for windfields using limited samples," *Wind Engineering*, vol. 42, no. 3, 2018, pp. 164–176.

[60] P. Martin and F. Rizzo, "Hypersingular integrals: how smooth must the density be?," *International Journal for Numerical Methods in Engineering*, vol. 39, no. 4, 1996, pp. 687–704.

[61] P. Martin, F. Rizzo, and T. Cruse, "Smoothness–relaxation strategies for singular and hypersingular integral equations," *International Journal for Numerical Methods in Engineering*, vol. 42, no. 5, 1998, pp. 885–906.

[62] S. Mukherjee, "CPV and HFP integrals and their applications in the boundary element method," *International Journal of Solids and Structures*, vol. 37, no. 45, 2000, pp. 6623–6634.

[63] S. Mukherjee, "Finite parts of singular and hypersingular integrals with irregular boundary source points," *Engineering Analysis with Boundary Elements*, vol. 24, no. 10, 2000, pp. 767–776.

[64] N. I. Muskhelishvili and J. R. M. Radok, *Singular integral equations: boundary problems of function theory and their application to mathematical physics*, Courier Corporation, 2008.

[65] P. J. Olver, *Introduction to partial differential equations*, Springer, 2016.

[66] P. Partheymüller, R. Białecki, and G. Kuhn, "Self-adapting algorithm for evaluation of weakly singular integrals arising in the boundary element method," *Engineering analysis with boundary elements*, vol. 14, no. 3, 1994, pp. 285–292.

[67] B. Plaza, R. Bardera, and S. Visiedo, "Comparison of BEM and CFD results for MEXICO rotor aerodynamics," *Journal of Wind Engineering and Industrial Aerodynamics*, vol. 145, 2015, pp. 115–122.

[68] A. Portela, M. Aliabadi, and D. Rooke, "The dual boundary element method: effective implementation for crack problems," *International Journal for Numerical Methods in Engineering*, vol. 33, no. 6, 1992, pp. 1269–1287.

[69] A. Portela, M. Aliabadi, and D. P. Rooke, "Dual boundary element incremental analysis of crack propagation," *Computers & Structures*, vol. 46, no. 2, 1993, pp. 237–247.

[70] T. S. Ribeiro, G. O. Ribeiro, and A. B. Jorge, "On the relaxed continuity approach for the selfregular traction-BIE," *Mecanica Computational*, vol. 21, 2002, pp. 1263–1281.

[71] J. Richardson, "Numerical p-version refinement studies for the regularized stress-BEM," *International journal for numerical methods in engineering*, vol. 58, no. 14, 2003, pp. 2161–2176.

[72] J. Richardson and S. Arjunon, "A p-Version of the Three-Dimensional Boundary Element Method," *Proceedings of the Huntsville Simulation Conference*, HSC 2009, pp. 281–288.

[73] J. Richardson and T. Cruse, "Weakly singular stress-BEM for 2D elastostatics," *International Journal for Numerical Methods in Engineering*, vol. 45, no. 1, 1999, pp. 13–35.

[74] J. Richardson, T. Cruse, and Q. Huang, "On the validity of conforming BEM algorithms for hypersingular boundary integral equations," *Computational Mechanics*, vol. 20, no. 3, 1997, pp. 213–220.

[75] J. Richardson, L. Gray, T. Kaplan, and J. Napier, "Regularized spectral multipole BEM for plane elasticity," *Engineering Analysis with Boundary Elements*, vol. 25, no. 4-5, 2001, pp. 297–311.

[76] F. Rizzo and D. Shippy, "An advanced boundary integral equation method for three-dimensional thermoelasticity," *International Journal for Numerical Methods in Engineering*, vol. 11, no. 11, 1977, pp. 1753–1768.

[77] F. J. Rizzo, "An integral equation approach to boundary value problems of classical elastostatics," *Quarterly of applied mathematics*, vol. 25, no. 1, 1967, pp. 83–95.

[78] T. Rudolphi, "The use of simple solutions in the regularization of hypersingular boundary integral equations," *Mathematical and Computer Modelling*, vol. 15, no. 3-5, 1991, pp. 269–278.

[79] P. Shah, C.-L. Tan, and X. Wang, "T-stress solutions for two-dimensional crack problems in anisotropic elasticity using the boundary element method," *Fatigue & Fracture of Engineering Materials & Structures*, vol. 29, no. 5, 2006, pp. 343–356.

[80] S. Sirtori, G. Maier, G. Novati, and S. Miccoli, "A galerkin symmetric boundary-element method in elasticity: Formulation and implementation," *International Journal for Numerical Methods in Engineering*, vol. 35, no. 2, 1992, pp. 255–282.

[81] J. Sladek and V. Sladek, "Regularized integral representation of thermoelastic stresses," *Engineering analysis with boundary elements*, vol. 8, no. 5, 1991, pp. 224–230.

[82] V. Sladek and J. Sladek, "Improved computation of stresses using the boundary element method," *Applied mathematical modelling*, vol. 10, no. 4, 1986, pp. 249–255.

[83] V. Sladek and J. Sladek, "Regularization of hypersingular integrals in BEM formulations using various kinds of continuous elements," *Engineering analysis with boundary elements*, vol. 17, no. 1, 1996, pp. 5–18.

[84] V. Sladek and J. Sladek, "Optimal coordinate transformations in numerical integrations of weakly singular and nearly singular integrals in BEMs," *WIT Transactions on Modelling and Simulation*, vol. 20, 1998.

[85] V. Sladek, J. Sladek, and M. Tanaka, "Regularization of hypersingular and nearly singular integrals in the potential theory and elasticity," *International Journal for Numerical Methods in Engineering*, vol. 36, no. 10, 1993, pp. 1609–1628.

[86] V. Sladek, J. Sladek, and M. Tanaka, "Evaluation of 1/r integrals in BEM formulations for 3-D problems using coordinate multitransformations," *Engineering analysis with boundary elements*, vol. 20, no. 3, 1997, pp. 229–244.

[87] V. Sladek, J. Sladek, and M. Tanaka, "Optimal transformations of the integration variables in computation of singular integrals in BEM," *International journal for numerical methods in engineering*, vol. 47, no. 7, 2000, pp. 1263–1283.

[88] V. Sladek, J. Sladek, and M. Tanaka, "Numerical integration of logarithmic and nearly logarithmic singularity in BEMs," *Applied mathematical modelling*, vol. 25, no. 11, 2001, pp. 901–922.

[89] A. Sutradhar, G. Paulino, and L. J. Gray, *Symmetric Galerkin boundary element method*, Springer Science & Business Media, 2008.

[90] J. Swedlow and T. Cruse, "Formulation of boundary integral equations for three-dimensional elasto-plastic flow," *International Journal of Solids and Structures*, vol. 7, no. 12, 1971, pp. 1673–1683.

[91] G. Symm, "Integral equation methods in potential theory. II," *Proceedings of the Royal Society of London. Series A. Mathematical and Physical Sciences*, vol. 275, no. 1360, 1963, pp. 33–46.

[92] M. Tanaka, V. Sladek, and J. Sladek, "Regularization techniques applied to boundary element methods," *Applied Mechanics Reviews*, vol. 47, no. 10, 1994, pp. 457–499.

[93] J. Telles, "A self-adaptive co-ordinate transformation for efficient numerical evaluation of general boundary element integrals," *International journal for numerical methods in engineering*, vol. 24, no. 5, 1987, pp. 959–973.

[94] W. Tsao and W. Hwang, "Regularized boundary integral methods for three-dimensional potential flows," *Engineering Analysis with Boundary Elements*, vol. 77, 2017, pp. 49–60.

[95] G. Xie, J. Zhang, X. Qin, and G. Li, "New variable transformations for evaluating nearly singular integrals in 2D boundary element method," *Engineering Analysis with Boundary Elements*, vol. 35, no. 6, 2011, pp. 811–817.

[96] J. Yu, *T-stress solutions of cracks emanating from ciruclar holes*, doctoral dissertation, Carleton University, 2006.

[97] Y. Zhang, Y. Gu, and J.-T. Chen, "Boundary element analysis of the thermal behaviour in thin-coated cutting tools," *Engineering analysis with boundary elements*, vol. 34, no. 9, 2010, pp. 775–784.

[98] Y.-M. Zhang, Y. Gu, and J.-T. Chen, "Boundary element analysis of 2D thin walled structures with high-order geometry elements using transformation," *Engineering analysis with boundary elements*, vol. 35, no. 3, 2011, pp. 581–586.

[99] M.-D. Zhu, "Duffy transformation with a simple polynomial smoothing strategy for weakly singular integrals," *Antennas and Propagation & USNC/URSI National Radio Science Meeting, 2017 IEEE International Symposium on*. IEEE, 2017, pp. 1569–1570.

[100] O. C. Zienkiewicz and R. L. Taylor, *The finite element method*, vol. 3, McGraw-hill London, 1977.